

AN ABSTRACT OF THE THESIS OF

Amar K. Kamadoli for the degree of Master of Science in  
Chemistry presented on May 8, 1992.

Title: Strontium Substitutions into the High-Temperature Tl/Ba/Ca/Cu/O  
2223 Superconductor.

Redacted for Privacy

Abstract approved: \_\_\_\_\_

Arthur W. Sleight

The  $Tl_2Ba_2Ca_2Cu_3O_{10}$  superconductor is well known for its claim to have the highest superconducting critical temperature,  $T_c$ , to date. Other high-temperature thallium cuprate superconductors also have been discovered in which strontium has been completely substituted for barium. Producing the phases responsible for superconductivity in these particular systems has been a challenge to researchers because of the many stringent synthesis conditions necessary for desired products. The experimental synthesis reactions can yield products that are single-phase or multi-phase, superconducting or not. The products from synthesis reactions that form in which the atoms have not gone to their correct sites, for ideal structures, often have lower  $T_c$ 's or can even be non-superconducting.

The main purpose of this study was to stoichiometrically dope strontium for calcium in the high-temperature Tl/Ba/Ca/Cu/O 2223-type superconductor systems. Strontium substitution studies were planned in an attempt to reduce the amount of site exchange between the cations of the Tl/Ba/Ca/Cu/O 2223-type superconductor systems. Many samples were prepared where different synthesis conditions were explored and the amount of strontium substitution was varied in the preparation of the Tl/Ba/Ca/Cu/O 2223-type systems. X-ray diffraction, magnetic susceptibility, and least-squares cell refinement were methods used to determine characteristics of the products.

The data collected from the analyses of the strontium-substituted products showed no trends nor enhancements with respect to the characteristics of the ideal 2223-type superconductor. Reproducibility of the data and results in many of the attempted systems of this study was limited, mostly due to the challenging nature of the experimental work itself.

**Strontium Substitutions into the High-Temperature  
Tl/Ba/Ca/Cu/O 2223 Superconductor**

by  
**Amar K. Kamadoli**

**A THESIS**  
submitted to  
**Oregon State University**

in partial fulfillment of  
the requirements for the  
degree of

**Master of Science**

**Completed May 8, 1992**

**Commencement June 1993**

APPROVED:

Redacted for Privacy

---

Professor of Chemistry in charge of major

Redacted for Privacy

---

Head of Department of Chemistry

Redacted for Privacy

---

Dean of Graduate School

Date thesis is presented: May 8, 1992

---

Typed by: Amar K. Kamadoli

---

## ACKNOWLEDGMENTS

I would like to thank my graduate advisor, Arthur W. Sleight, for his assistance, support, and counsel in my graduate training. I am very grateful to my graduate committee of Micheal M. Lerner (inorganic chemistry), Douglas A. Keszler (inorganic chemistry), Phillip R. Watson (physical chemistry), and Chih-An Huh (oceanography) for their valuable comments, criticism, questions, suggestions, guidance, and ideas in the development of this thesis.

I am grateful to Jinfan Huang for the numerous and insightful discussions, and especially for challenging me to become a better scientist. I thank Vince Korthius, Phong Nguyen, and the other graduate students in the Sleight Lab for their comradeship through graduate school and their helpful assistance in various laboratory and computer projects.

I would like to express much gratitude, appreciation, and my deepest thanks to Rolf-Dieter Hoffmann for the enlightening discussions in the laboratory and at lunches, for his generous assistance that often was above and beyond the call of duty, and for a friendship that I shall not forget.

I also would like to thank many other friends, related and unrelated to my graduate work, whom with I shared many memorable times and will remember for years to come.

I am especially thankful to my parents and family for their time, understanding, patience, support, and encouragement throughout all the

years of my education. For without them, much of what I have accomplished would not have been possible.

Finally, a special acknowledgment to Terry Shrout, Judy Armstrong, James Borsberry, Mont Rock, Dwight Runner, Christina Brink, Frances Chapple, Norman Hudak, David Goodney, and many other chemistry and science educators, whom over many years have supported, inspired, challenged, and encouraged me along the pathways to ever higher levels of scientific knowledge and understanding.

## TABLE OF CONTENTS

INTRODUCTION	1
EXPERIMENTAL DETAILS	9
RESULTS AND DISCUSSION	21
The $Tl_2Ba_2Ca_{1.5}Sr_{0.5}Cu_3O_y$ system	21
The $Tl_2Ba_2Ca_{2-x}Sr_xCu_3O_y$ systems	27
The $Tl_2Ba_2Ca_3Cu_4O_{12}$ and $Tl_2Ba_2Ca_{3-x}Sr_xCu_4O_y$ systems	31
The $Tl_2Ba_2Ca_{2+x}Cu_{3+x}O_y$ systems	41
The $Tl_2Ba_2Ca_{2.5-x}Sr_xCu_{3.5}O_y$ systems	46
Post-synthesis annealing treatment	51
Least-Squares Cell Refinement	54
SUMMARY AND CONCLUSIONS	59
BIBLIOGRAPHY	63
APPENDICES	66
Appendix 1. Theoretical X-ray diffraction pattern of $Tl_2Ba_2Ca_2Cu_3O_{10}$	66
References	67
Appendix 2. Volume and mass magnetic susceptibilities	68
References	71
Appendix 3. Relationship of measured voltage and susceptibility in the Lake Shore 7000 AC Susceptometer	72
References	74

## LIST OF FIGURES

<u>Figure</u>		<u>Page</u>
1.	Copper oxide sheet arrangement	3
2.	The $Tl_2Ba_2Ca_2Cu_3O_{10}$ structure	4
3.	Cross-sectional of susceptometer coils	16
4.	Magnetic susceptibility versus temperature plot	20
5.	X-ray diffraction pattern #1 of $Tl_2Ba_2Ca_{1.5}Sr_{0.5}Cu_3O_y$	23
6.	Magnetic susceptibility of $Tl_2Ba_2Ca_{1.5}Sr_{0.5}Cu_3O_y$	24
7.	X-ray diffraction pattern #2 of $Tl_2Ba_2Ca_{1.5}Sr_{0.5}Cu_3O_y$	26
8.	X-ray diffraction pattern of $Tl_2Ba_2Ca_{1.85}Sr_{0.15}Cu_3O_y$	30
9.	X-ray diffraction pattern of $Tl_2Ba_2Ca_3Cu_4O_{12}$	33
10.	X-ray diffraction pattern of $Tl_2Ba_2Ca_{2.85}Sr_{0.15}Cu_4O_y$	39
11.	Magnetic susceptibility of $Tl_2Ba_2Ca_{2.85}Sr_{0.15}Cu_4O_y$	40
12.	X-ray diffraction pattern of $Tl_2Ba_2Ca_{2.5}Cu_{3.5}O_y$	44
13.	Magnetic susceptibility of $Tl_2Ba_2Ca_{2.5}Cu_{3.5}O_y$	45
14.	Annealed $Tl_2Ba_2Ca_{1.5}Sr_{0.5}Cu_3O_y$ X-ray pattern	53
15.	X-ray diffraction pattern of $Tl_2Ba_2Ca_2Cu_3O_{10}$	66

## LIST OF TABLES

<u>Table</u>	<u>Page</u>
1. The $Tl_2Ba_2Ca_{2-x}Sr_xCu_3O_y$ series	29
2. Products of the $Tl_2Ba_2(Ca_{0.85}Sr_{0.15})_{x-1}Cu_xO_y$ series	36
3. The $Tl_2Ba_2Ca_{3-x}Sr_xCu_4O_y$ series	37
4. The $Tl_2Ba_2Ca_{2+x}Cu_{3+x}O_y$ series	42
5. The $Tl_2Ba_2Ca_{2.5-x}Sr_xCu_{3.5}O_y$ series	47
6. $Tl_2Ba_2Ca_{2.5-x}Sr_xCu_{3.5}O_y$ heating time and $T_c$ data	50
7. $Tl_2Ba_2Ca_{2+x}Cu_{3+x}O_y$ refined <i>c</i> -axis cell dimensions	57
8. $Tl_2Ba_2Ca_{2.5-x}Sr_xCu_{3.5}O_y$ refined <i>c</i> -axis cell dimensions	58

## STRONTIUM SUBSTITUTIONS INTO THE HIGH-TEMPERATURE

### Tl/Ba/Ca/Cu/O 2223 SUPERCONDUCTOR

#### INTRODUCTION

The discovery of high-temperature superconductivity in oxides during the 1980's has led to many intensive studies of the superconducting systems.<sup>1</sup> The copper oxide superconductors have gained much attention in the last decade by possessing many of the highest known superconducting critical temperatures ( $T_C$ ) to date. Interest in high temperature superconductivity grew even more when the 1-2-3 Y/Ba/Cu oxide showed evidence of  $T_C$ 's above the temperature of liquid nitrogen.<sup>2</sup> Compounds containing Bi/Sr/Cu/O<sup>3</sup> and Tl/Ba/Cu/O<sup>4</sup> provided some of the first steps toward the greatest advances seen in oxide superconductivity since the mid-1970's. In 1987 and early 1988, visions of feasible room-temperature superconductors were discussed among scientists when  $T_C$ 's were reported in the Bi/Sr/Ca/Cu/O system as high as 90K,<sup>5</sup> and in the Tl/Ba/Ca/Cu/O system over the 100K mark.<sup>6-9</sup> Efforts in the field of superconductivity increased dramatically as many scientists and laboratories attempted to prepare single-phase samples that contained the phases accountable for the phenomenon of superconductivity.

The bismuth and thallium high- $T_C$  superconductors are generally represented by the formula of  $A_m M_2 Ca_{n-1} Cu_n O_{2n+m+2}$ . In the case of the thallium systems,  $A = Tl$  and  $M = Ba$ , with  $TlBa_2Ca_{n-1}Cu_nO_{2n+3}$  where  $m = 1$  and  $n$  ranges from 1 to 6, and  $Tl_2Ba_2Ca_{n-1}Cu_nO_{2n+4}$  where  $m = 2$  and  $n$

ranges from 1 to 4. The thallium system where  $m = 2$  and  $n = 3$  represents the  $Tl_2Ba_2Ca_2Cu_3O_{10}$  compound, or more commonly referred to as the 2223 compound or structure. The highest known  $T_C$  of 125K is held by the 2223 compound.<sup>9</sup>

Figure 1 on page 3 shows a copper oxide sheet, which can be thought of as  $CuO_4$  square-planar units linked together through the oxygen atoms. The  $CuO_4$  sheets are the characteristic feature of the copper oxide superconductors. The sets of triply-stacked consecutive copper oxide sheets in the 2223 superconductor represent a rigid and covalent network of the linked and layered  $CuO_4$  units.

Initial studies of the thallium cuprates predicted that the system of  $Tl_2Ba_2Ca_{n-1}Cu_nO_{2n+4}$  would have successively higher  $T_C$ 's that correlated with increasing  $n$ ,<sup>7</sup> where  $n$  represents the number of consecutively stacked copper oxide sheets present in the phase. This held true for  $n = 1$  to 3, however the assumption collapsed as  $n$  with more than three copper oxide layers revealed lower  $T_C$ 's when these compounds were synthesized and tested.<sup>10,11</sup>

Studies of the  $Tl_2Ba_2Ca_{n-1}Cu_nO_{2n+4}$  structures brought forth some of the first understandings of the 2223 structure.<sup>8,12,13</sup> The  $Tl_2Ba_2Ca_{n-1}Cu_nO_{2n+4}$  structures differ from one another primarily in the number of consecutively stacked copper oxide sheets. The 2223 three-layer copper oxide structure in Figure 2 on page 4 contains triple sheets of square-planar corner-sharing  $CuO_4$  groups oriented parallel to the (001) plane.

Additional oxygen atoms are located above and below the triple copper oxide sheets and are positioned at a distance of 2.5 Å from the copper

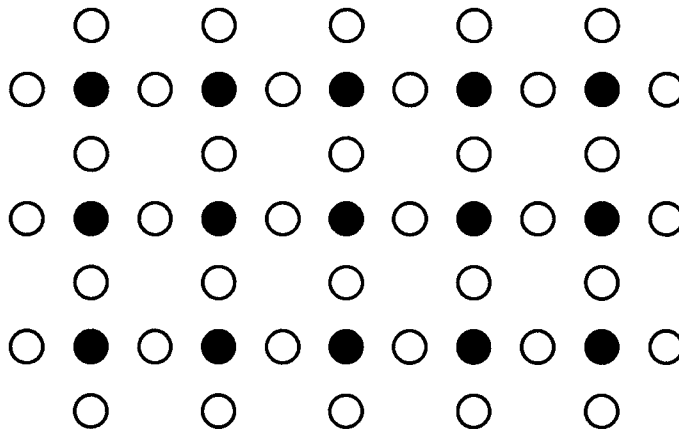


Figure 1. Copper oxide sheet arrangement. This representation shows the sheet in the plane of the paper. The filled circles are copper and the open circles are oxygen.

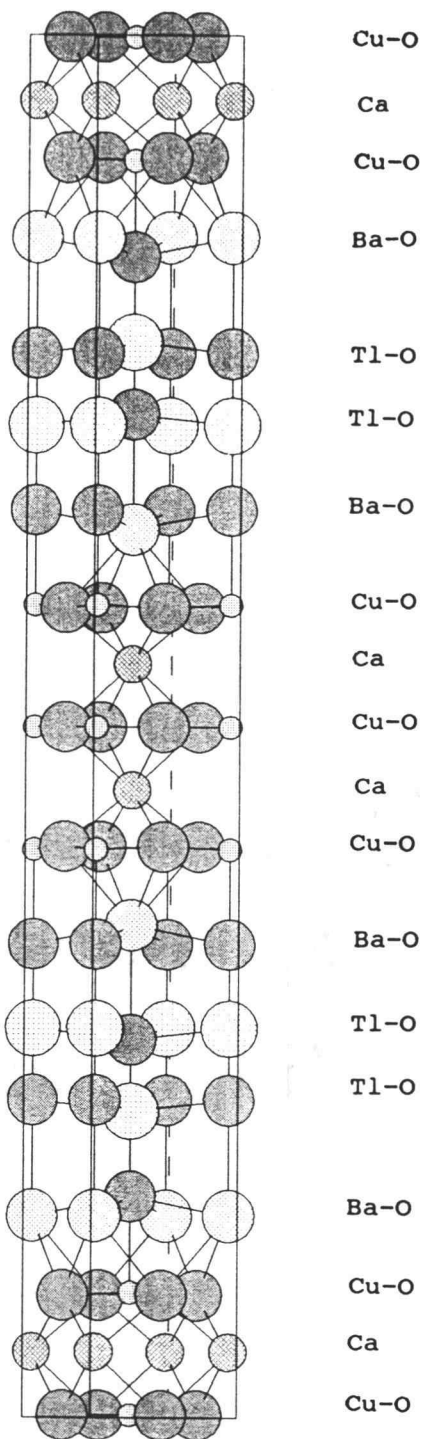


Figure 2. The  $\text{Tl}_2\text{Ba}_2\text{Ca}_2\text{Cu}_3\text{O}_{10}$  structure. Commonly referred to as the 2223 structure. The unit cell is tetragonal and has the dimensions of  $a = 3.85 \text{ \AA}$  and  $c = 35.88 \text{ \AA}$ .

atoms. There are no oxygen atoms located between the copper oxide sheets in the 2223 structure, unlike the similar two-layer copper oxide superconductor,  $\text{Tl}_2\text{Ba}_2\text{CaCu}_2\text{O}_8$  (also known as the 2212 structure). The copper-oxygen bonds in the sheets of the 2223 have been determined to be 1.925 Å in the middle sheet and 1.927 Å in the two outer sheets. The individual copper oxide sheets are separated by 3.2 Å, when measured from copper to copper. Calcium ions coordinate to eight oxygen atoms with  $C_{4v}$  site symmetry and an average calcium-oxygen distance of 2.48 Å. The barium ions are located just above and below the set of triply-stacked copper oxide sheets and are nine-coordinated with oxygen. Thallium bonds to six oxygen atoms in a distorted octahedral arrangement where the octahedra share edges within the *ab* plane. Considering all the atoms and the copper oxide sheet arrangement of the 2223 structure, the layering sequence is ---Tl-Tl-Ba-Cu-Ca-Cu-Ca-Cu-Ba--- along the *z* direction or long axis of the unit cell. The middle copper oxide sheet is constrained by symmetry to be flat, however, the two outer copper oxide sheets are slightly buckled.

The Tl/Ba/Ca/Cu/O 2223 symmetry is tetragonal and is in the space group  $I4/mmm$ , number 139. The refined unit-cell dimensions calculated by Torardi *et al.* are 3.85 Å for the *a*-axis and 35.88 Å for the *c*-axis.<sup>8</sup> The other two superconductors in the  $\text{Tl}_2\text{Ba}_2\text{Ca}_{n-1}\text{Cu}_n\text{O}_{2n+4}$  systems,  $\text{Tl}_2\text{Ba}_2\text{CuO}_6$  (2201 structure), and  $\text{Tl}_2\text{Ba}_2\text{CaCu}_2\text{O}_8$  (2212 structure) are also tetragonal and have essentially similar *a*-axis dimensions compared to the 2223 structure, being 3.87 Å and 3.85 Å, respectively. The 2201 and the 2212 structures have *c*-axis cell dimensions of 23.24 Å and 29.42 Å, respectively.<sup>12,13</sup>

The occupation factors for the metal atoms, also refined by Torardi *et al.*,<sup>8</sup> were found to be low for thallium and high for calcium, indicating substitution of thallium on the calcium site. The level of substitution determined gave a 15% occupancy of calcium on the thallium site, and a 12% occupancy of thallium on the calcium site. The study by Torardi *et al.* also mentioned that it was difficult to conclude whether or not the thallium sites were fully occupied. A comparison of ionic radii for thallium, barium, and calcium (0.98 Å, 1.35 Å, and 1.12 Å, respectively)<sup>14</sup> shows that partial occupancy of thallium on the calcium site is a reasonable assumption. The opportunity for thallium and calcium to occupy the "incorrect" site due to substitution leads to many product stoichiometries different from the ideal 2223 phase.

The first reported synthesis of a high-temperature superconductor in the Tl/Ba/Ca/Cu/O system was by Sheng and Hermann in early 1988.<sup>6</sup> The methods these researchers used to synthesize the phase accountable for high-temperature superconductivity were to 1) mix and grind the reagent oxide powders, 2) press the powders into a pellet, 3) put the pellet into a tube furnace pre-heated to 880-910°C for 3-5 minutes in flowing oxygen, 4) then remove the pellet from the furnace and quench it to room temperature in air. Their methods of synthesis resulted in products of many mixed phases and broad superconducting temperature transition regions of up to 20K. It is true that part of the product Sheng and Hermann synthesized did exhibit a  $T_c$  of over 120K, however, there were other phases, many of which were non-superconducting or superconducting at lower temperatures, that formed with the superconducting phases in the total product. With non-sealed reactions (non-hermetic) the chance of obtaining high- $T_c$  phases in the bulk of the

product is low, while the chances for the formation of mixed phases and the inter-growth of mixed phases are great.

Soon thereafter, synthetic methods that maximize the formation of the highest-temperature superconducting phase were developed. The methods employed aimed at producing the high- $T_C$  phase in the bulk of the product rather than as a minor portion of the product. Hermetically-sealed systems were found to work well because they minimized the thallium loss during the heating period.<sup>8,13,15</sup> (Thallium is extremely volatile at synthesis temperatures)

Strontium is also a component of several copper oxide superconductor systems. Research efforts with strontium in the Bi/Sr/Ca/Cu oxides have revealed  $T_C$ 's that approach 110K.<sup>5</sup> Strontium has also been substituted into barium-absent thallium cuprates with the general formula of  $TlSr_2Ca_{n-1}Cu_nO_{2n+3}$ , and the products show  $T_C$ 's up to 123K.<sup>16,17</sup>

It may be possible that strontium can be used in the 2223 Tl/Ba/Ca/Cu/O system to reduce the site exchange between thallium and calcium. Strontium and calcium have ionic radii of 1.12 Å and 0.99 Å, respectively.<sup>14</sup> Considering the small size difference between strontium and calcium, it is possible that strontium can fit onto the calcium sites if strontium is partially substituted (doped) in for calcium. If strontium is a competing species for the calcium sites, thallium would be less likely to occupy the calcium sites. This is not to argue that calcium and thallium site exchange would not occur, however the exchange for the other site would be less than if strontium were not present. Barium has an ionic radius of 1.34 Å, which is larger than the ionic radii of thallium, calcium, and strontium.<sup>14</sup> Barium will not favorably

substitute onto the calcium sites given its larger atomic radius. Therefore, the chances of strontium substituting onto calcium sites would be more favorable than of barium substituting onto the calcium sites.

The discovery of the 2223 system has prompted many studies to see if further research in the field of thallium cuprates might yield superconductors with even higher critical temperatures. Scientists have been attempting various synthetic methods, techniques, and elemental substitutions in a hope to reach higher  $T_c$ 's, and to obtain more information about structural, magnetic, and electronic properties of these systems.

Synthesizing thallium cuprate superconductors has been an ongoing challenge to researchers in the scientific field. The conditions required to form the superconducting phases can be very stringent and often necessitate careful and meticulous preparation techniques and skills for the experimental scientist. Reagent stoichiometries, reaction conditions, and post-synthesis treatment are considerations that are very important in obtaining successful and worthy results in the field of copper oxide superconductors.

The purposes of this study were the following: 1) to attempt to partially substitute strontium for calcium in the Tl/Ba/Ca/Cu/O 2223-type structure, 2) to find optimum synthetic techniques, conditions, reactions, and preparatory schemes for strontium substitutions, and 3) to find new strontium-substituted superconductors with even higher  $T_c$ 's, based on the thallium cuprate 2223-type structure.

## EXPERIMENTAL DETAILS

The superconductors in this study were prepared through solid state techniques. The reagents used were  $Tl_2O_3$ , 99.999% (Johnson Matthey);  $BaO_2$ , 97.7% (Baker);  $CaO$  (Baker);  $CaO_2$ , technical grade (Pfaltz & Bauer);  $SrO_2$ , 95% (Pfaltz & Bauer);  $SrCO_3$ , 99.9% (Baker);  $CuO$ , 99.9% (Baker). The  $SrCO_3$  reagent was used in the initial stages of this study until  $SrO_2$  was realized to be a more convenient reagent. Preparation of compounds using  $SrCO_3$  required an extra heating step in the synthesis. Pre-heating of  $SrCO_3$  was necessary to drive off  $CO_2(g)$  to obtain  $SrO$ , which is preferred for a hermetically-sealed solid state reaction. Strontium peroxide,  $SrO_2$ , was used essentially for all the experiments of this study except for a few experiments at the beginning of the study.  $SrO_2$  was used as a reagent for the experiments directly as supplied without any special pre-preparation.

For sample preparations the reagent oxides were thoroughly mixed and ground together using an agate mortar and pestle. Whenever possible, mixing and grinding were performed under a fume hood to minimize human exposure to thallium. Extreme care must be taken when working with thallium due of the toxicity of  $Tl_2O_3$ . Latex gloves, eye protection, and other safety gear and habits were employed as necessary to reduce thallium inhalation, contact, and absorption through the skin.

Following the preparation of a singly-mixed and well-ground powder, each powder sample was pressed into a cylindrical pellet under a force of five to six tons using a hydraulic hand press and a one-quarter inch tungsten carbide die set. The pressed pellets were cut into small

pieces or "shards" using a razor blade. Cutting the pellet into shards allowed the thin shard pieces to fit into the approximately 5 mm diameter reaction tube containers.

The reaction tubes were made of high-purity gold or silver. Gold and silver are the container materials of choice in the synthesis of thallium cuprate superconductors because of their relatively high melting points (961°C for silver, 1064°C for gold) and low reactivity with the reagents. Silica is not an ideal container because it is attacked by thallium and the peroxides ( $\text{CaO}_2$  and  $\text{BaO}_2$ ) under the heating conditions needed for the synthesis of the 2223 superconductor systems.

Gold tubing was used exclusively as a reaction container from the beginning of this study until it was later determined that silver tubing of comparable size performed nearly as well. However, using silver tubing limited the range of synthesis heating temperatures to less than 875°C. Heating silver tubing beyond 875°C subjected the tube to much fatigue very rapidly during the heating period. Gold tubing was used without many problems up to temperatures of 925°C. Although higher temperatures probably could have been sustained by gold tubing, the maximum reaction temperature that could be sustained by the reagent oxide powders was the factor that limited the maximum heating temperature. It should be mentioned that because silver is inexpensive compared with gold, much more silver tubing was purchased and used for the experimental studies than was gold tubing.

All gold and silver tubing were prepared for use by thoroughly cleaning the tubing with an aqueous soap solution, followed by drying, and rinsing with acetone. After the acetone rinsing, the tubes were quickly pre-heated with a torch using a moderate flame. The tubes were

cut with metal shears so that the tube lengths ranged from about two to seven centimeters. For each cut piece of tubing, one end was carefully crimped with flat-tipped pliers and carefully heat sealed using an  $H_2/O_2$  gas torch, to melt the crimp shut.

The sample shards were then inserted into the tubing. Each tube was filled to about half of the tube capacity, regardless of the tube length. When samples were prepared in a series, for example, when systematically increasing the strontium doping level or stoichiometry in each successive sample, the tubes for the series were selected to be as similar in length as possible and approximately the same amount of sample was placed in each sample tube. The total mass of reagents (shards) put into a single tube was approximately a gram or less.

Hermetically sealing the tube, using a torch, has been demonstrated to be a very successful method to achieve optimal results in synthesizing the 2223 superconductor systems. However, certain precautions must be taken in order to achieve a satisfactory seal. It is important that the sample within the tubing not be selectively heated to high temperatures (one end of the tube being heated more than the other) or overheated when melting shut the second crimp. To prevent any heating problems while melting shut the second crimp, the sample tube was held in a beaker of water using pliers so that the first-crimped end and most of the tube was below the water and the second-crimped end was just above the water surface. The  $H_2/O_2$  flame was then passed over the second crimp and any excess heat applied to the tube while melting shut the crimp would be dissipated to the water as much as possible. Excessive pressure build-up inside the tube while heat sealing the second crimp shut was not a major concern because the torch was hot

enough so that only a few quick passes of the flame over the end of the tube were needed to melt the second crimp shut.

The prepared hermetically-sealed tube was then placed into a furnace for the heating of the sample. In some cases, many samples (sometimes up to five or ten samples) were put simultaneously into the same furnace in order to heat similarly prepared samples under as close to identical heating conditions as possible. A Thermolyne Type 48000 furnace with electronic temperature program capability was used for the heating of all the samples in this study. This furnace was dedicated to heat any samples containing thallium and was located under a fume hood, therefore minimizing the possibility of thallium exposure and limiting any possible thallium contamination to just a single laboratory furnace. Heating rates, dwell times, set-point temperatures, cooling rates, and other furnace parameters were programmed into the electronic control for each heating run. The parameters were changed as needed for the various samples of this study. The samples were placed in the center floor area of the furnace for each run, thus maintaining the best chance for heating reproducibility while not having the sample tubes located too close to either of the two side-wall heating elements.

Upon completion of a given furnace program, the sample tubes were removed from the furnace and inspected for signs of reagent or product leakage, or both. The tubes were also checked for holes, cracks, tube fatigue, and other problems that may have occurred during the heating period. After any problems were noted from the heating period, the tubes were then cut open at one end with metal shears. The product shards were removed from the tubing and placed in a sample vial. The opened tubing was then placed in a beaker of acid for cleaning. Nitric

acid was used to clean the gold tubing and hydrochloric acid was used to clean the silver tubing. The tubing was allowed to soak completely in their respective acid for at least a day for a thorough cleaning. Later, the tubing was removed from the acid, rinsed and cleaned as mentioned above, and reused for a future sample. It was possible to get several experimental runs with the same piece of tubing, just as long as the tube did not develop any cracks, large holes, or collapse from overheating.

The sample shards that were removed from the opened tubing first were visually inspected with a microscope to check for any possible single crystal formation in the product. The sample was then ground into a fine powder using an agate mortar and pestle.

Powder X-ray diffraction was the primary method used to determine the phases present in the product, the structural nature of the product, and any impurity and reagent phases that may be present in the product. Powder X-ray diffraction data were collected for all samples using a Siemens D5000 X-ray diffractometer. X-ray diffraction data were usually collected from  $2^{\circ}$  to  $60^{\circ}$  two-theta in  $0.02^{\circ}$  steps. Counting times for X-ray diffraction were chosen differently for samples depending on what information was needed. Scans necessary for least-squares unit cell refinement with an internal standard usually required long counting times to obtain good data statistics. Sample scans of smaller two-theta scan ranges and shorter counting times were used more often for qualitative purposes. The qualitative scans were performed to determine the presence and character of the low-angle diffraction peaks, usually in the range of  $2^{\circ}$  to  $12^{\circ}$  two-theta. Standard silicon X-ray diffraction powder (National Bureau of Standards grade) was used for all samples

analyzed with an internal standard. Least-squares unit cell refinement was performed with computer software supplied with the Siemens D5000 X-ray diffractometer software package.

Figure 15 in Appendix 1 (page 66) is an example of a powder X-ray diffraction pattern. This particular X-ray diffraction pattern is of the  $Tl_2Ba_2Ca_2Cu_3O_{10}$  structure based on the atomic positions refined and reported by Torardi *et al.*<sup>8</sup> The pattern in Figure 15 was generated by the Rietveld analysis computer program Rietan, a program that was developed by Izumi.<sup>18,19,20</sup>

An alternating current (AC) susceptometer was used for the determination of the magnetic characteristics of many products. The susceptibility that is experimentally measured is actually volume magnetic susceptibility, however, mass magnetic susceptibility is related to volume magnetic susceptibility and can be calculated directly from the volume magnetic susceptibility. The computer software used with the AC susceptometer was capable to directly calculate mass magnetic susceptibility. Appendix 2 further explains the details and relationship between volume magnetic susceptibility and mass magnetic susceptibility. In this study the term "magnetic susceptibility" is meant to imply "mass magnetic susceptibility."

Magnetic susceptibility data were collected using a Lake Shore 7000 Alternating Current Susceptometer. The AC susceptometer, its theory and method of operation in magnetic susceptibility measurements can be explained briefly. A powder sample of about 0.3 gram was put into a 3.6 mm diameter by 13 mm long cylindrical sample holder and attached to the end of a long metal rod. The metal rod was then inserted down into the cryostat of the susceptometer where temperature,

atmosphere, pressure (pressures lower than atmospheric only), and magnetic fields are controlled. The upper end of the rod was connected to a motor that raised and lowered the sample holder during the measurement.

Figure 3 on page 16 shows the two sets of coils that surround the sample, a primary coil and two secondary coils, and the sample holder connected to the lower end of the metal rod. The cylindrical primary coil generates the alternating magnetic field to which the sample is subjected. The secondary coils are concentrically arranged within the primary coil and one secondary coil is located above the other secondary coil. The secondary coils are electrically connected in opposition in order to cancel the voltages induced by the AC field itself or voltages induced by unwanted external sources.

The sample was flushed with helium gas a few times before the magnetic susceptibility measurement. Atmospheric oxygen needed to be evacuated prior to sample measurement because it is paramagnetic and could have condensed on the sample at temperatures below 90K. Throughout the magnetic susceptibility measurement an atmosphere of helium gas always surrounded the sample. The liquid nitrogen that was contained in the dewar cooled the helium gas, and the gas in turn cooled the sample. Once the sample had cooled to the desired temperature to begin a measurement (at least 90K), the software on the computer that controls the susceptometer was programmed with the parameters needed to collect magnetic susceptibility data for the sample.

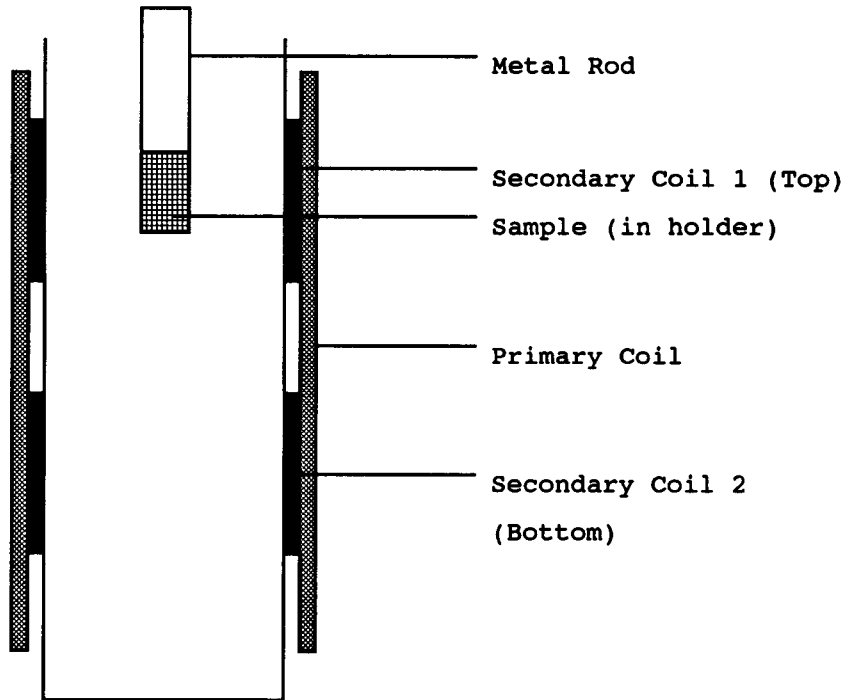


Figure 3. Cross-sectional of susceptometer coils. This figure shows the sample at the top secondary coil (#1). The metal rod moves the sample vertically between the two different secondary coils.

When the software was fully configured (this was done before the sample had cooled to the experiment starting temperature) it began with user command. The software controlled many important aspects during a measurement, including 1) the alternating current in the primary coil surrounding the sample, 2) the heating rate of the sample, 3) the sample movement between the two secondary coils, and 4) the data collection.

The sample was moved vertically between the two secondary coils at a rate of one "up and down" cycle about every minute. The rate of heating was typically 1.0K to 1.5K per minute. Magnetic susceptibility data were collected from at least 90K to about 120-130K for each sample.

Throughout the entire magnetic susceptibility experiment, the sample was subjected to a small alternating magnetic field of 100 Hz. The flux variation due to the sample was picked up by one of the two secondary sensing coils (the appropriate sensing coil takes the measurement depending on whether the sample is in the "up" or "down" position) surrounding the sample and the resulting voltage induced by the coil was detected. The measured voltage is directly proportional to the (volume) magnetic susceptibility of the sample. The software was programmed to calculate and convert the measured voltages to susceptibility based on the mass of the sample. The data for the susceptibility were stored in a computer file and the file output consisted of measured temperature and magnetic susceptibility data. Appendix 3 contains further details on voltage to susceptibility calculations.

The data from the AC susceptometer files were used with a computer spreadsheet program to determine the  $T_c$ 's of the measured samples. One unique property of a superconductor is its diamagnetic state.

Diamagnetism is measured as a negative magnetic susceptibility (and by similar reasoning, paramagnetism is measured as a positive magnetic susceptibility).

The thallium cuprate systems tested in this study for superconductivity are diamagnetic when superconducting and are anti-ferromagnetic when not superconducting, or insulating. Anti-ferromagnetism is seen as a zero voltage in a susceptometer measurement and therefore, measured susceptibility calculates to be zero. Figure 4 on page 20 shows a typical magnetic susceptibility versus temperature plot. The  $T_c$  shown in this figure is 112K. In Figure 4, the susceptibility is negative (the sample is diamagnetic and superconducting) below  $T_c$ , and the susceptibility is zero (the sample is anti-ferromagnetic and insulating) at and above  $T_c$ .

Post-synthesis annealing studies were done in a tube furnace at lower temperatures, typically in the range of 300°C to 400°C. Powder samples were placed in open alumina boat-type crucibles and allowed to heat in the tube furnace while in the flow of annealing gases. The gases used in post-synthetic annealing treatment were either safe  $H_2(g)$  ( $H_2$  diluted with argon gas),  $N_2(g)$ , or  $O_2(g)$ , depending on whether reducing or oxidizing conditions were attempted.

Open-ended silica tubing was used in the latter part of this study to serve as a qualitative monitor of thallium leakage from the reaction container (silver) tubing during the furnace heating programs. A hermetically-sealed sample container tube was placed so that it was lying within a larger diameter silica tubing that completely encircled the sample container tubing. A single silica tube was used for each silver container tube. Thallium reacts with silica at elevated

temperatures and thus leaves evidence of even the smallest amounts of thallium leakage, including thallium vapors that may leak from the "sealed" sample container tube. In many instances no visible holes were seen in the sample container tubing after a sample heating run, however, leakage did often occur, and to varying extent during the high-temperature heating of the sample reagents.

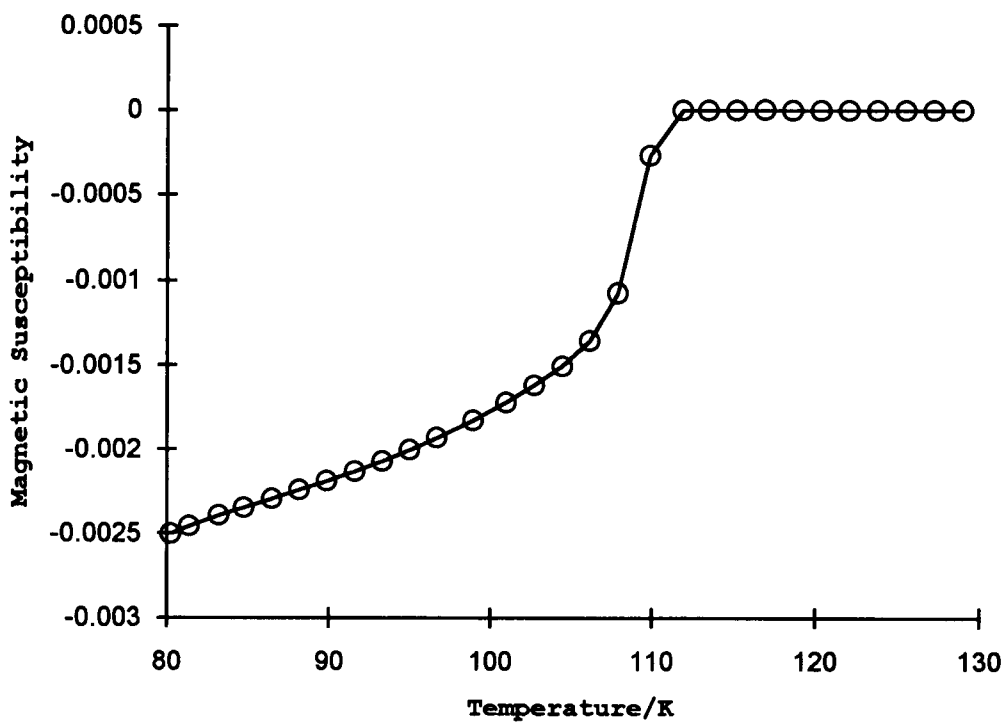


Figure 4. Magnetic susceptibility versus temperature plot. This shows the superconducting critical temperature,  $T_C$ , to be 112K. Below 112K the susceptibility is negative, thus indicating diamagnetism in the sample. At 112K and above the susceptibility is zero, indicating anti-ferromagnetism in the sample. Only below 112K is the sample superconducting. At 112K and above, it is insulating.

## RESULTS AND DISCUSSION

**The  $Tl_2Ba_2Ca_{1.5}Sr_{0.5}Cu_3O_y$  system**

The first strontium substituted 2223 Tl/Ba/Ca/Cu/O superconductors attempted in this study were of the starting composition  $Tl_2Ba_2Ca_{1.5}Sr_{0.5}Cu_3O_y$ . The reagents included  $Tl_2O_3$ ,  $BaO_2$ ,  $CaO$ ,  $SrCO_3$ , and  $CuO$ . Gold tubing was used for the containers in these reactions. The reactants were prepared as specified in the experimental section with the following modifications. When the reactant shards were placed into the gold tubing (with one end of the tube already heat-sealed), the tube and the reactant shards were subjected to an "initial" heating period to drive off  $CO_2(g)$  from the  $SrCO_3$  reagent. This was accomplished by placing the open tube with reagent contents into a furnace that was programmed to ramp from room temperature to  $790^\circ C$  at the maximum furnace heating rate. The time it took the furnace to ramp from room temperature to  $790^\circ C$  was about 35 to 40 minutes. When the temperature of  $790^\circ C$  was reached, the furnace door was immediately opened and the open sample tube with contents was quickly removed to room temperature. Note: This method of pre-heating the reagents presents a potential for much thallium loss due to the volatility of  $Tl_2O_3$  at low temperatures.  $Tl_2O_3$  begins to lose oxygen at about  $100^\circ C$  and the conversion to  $Tl_2O(g)$  and  $O_2(g)$  is complete at  $875^\circ C$  in air.<sup>21</sup>

Following the "initial" heating to drive off as much carbon dioxide as possible while minimizing thallium loss, the open end of the tube was crimped flat with pliers and the crimp was melted shut using an

H<sub>2</sub>/O<sub>2</sub> torch. When the furnace had cooled to room temperature, after the initial heating period, the sealed gold tube was placed in the center of the furnace (floor area) for the second heating. The tubing was oriented so that it was horizontally-positioned on the bottom surface of the furnace.

Of the samples that were initially heated with the tube open, many of the products were multi-phase. Figure 5 on page 23 shows a powder X-ray diffraction pattern of one of the Tl<sub>2</sub>Ba<sub>2</sub>Ca<sub>1.5</sub>Sr<sub>0.5</sub>Cu<sub>3</sub>O<sub>y</sub> systems synthesized with SrCO<sub>3</sub> and the experimental methods noted above. The figure is also highly representative of many Tl<sub>2</sub>Ba<sub>2</sub>Ca<sub>1.5</sub>Sr<sub>0.5</sub>Cu<sub>3</sub>O<sub>y</sub> systems that exhibited two-layer and three-layer multi-phase products. Figure 6 on page 24 shows an example of a magnetic susceptibility versus temperature plot of a two-layer and three-layer multi-phase Tl<sub>2</sub>Ba<sub>2</sub>Ca<sub>1.5</sub>Sr<sub>0.5</sub>Cu<sub>3</sub>O<sub>y</sub> product. This particular Tl<sub>2</sub>Ba<sub>2</sub>Ca<sub>1.5</sub>Sr<sub>0.5</sub>Cu<sub>3</sub>O<sub>y</sub> product exhibited one of the highest observed T<sub>C</sub>'s in the Tl<sub>2</sub>Ba<sub>2</sub>Ca<sub>1.5</sub>Sr<sub>0.5</sub>Cu<sub>3</sub>O<sub>y</sub> system, measured to be 117K. Another phase transition is also observed around 97-105K, as evidenced by the subtle plateau and change in curvature of the magnetic susceptibility versus temperature plot. The figure shows that the three-layer phase is superconducting below 117K, and the two-layer phase becomes superconducting below the 97-105K temperature region.

After synthesizing some Tl<sub>2</sub>Ba<sub>2</sub>Ca<sub>1.5</sub>Sr<sub>0.5</sub>Cu<sub>3</sub>O<sub>y</sub> systems using SrCO<sub>3</sub> as a reagent and having products mostly of two-layer and three-layer compositions, it was decided that SrO<sub>2</sub> would be used as a reagent so that the "initial" heating period could be eliminated. When using SrO<sub>2</sub> as a reagent, all the metal oxides were mixed and ground together, pressed into a pellet, cut into shards, inserted and heat sealed into a

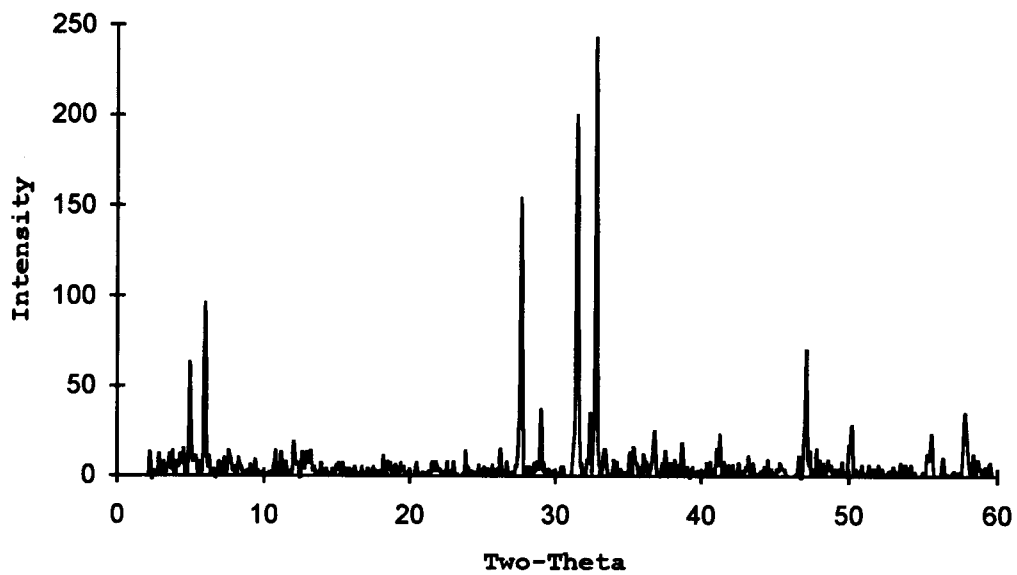


Figure 5. X-ray diffraction pattern #1 of  $\text{Tl}_2\text{Ba}_2\text{Ca}_{1.5}\text{Sr}_{0.5}\text{Cu}_3\text{O}_y$ .  $\text{SrCO}_3$  was used as a reagent. The two sharp peaks at approximately  $5^\circ$  and  $6^\circ$  two-theta indicate the 002 phases of the three-layer and two-layer copper oxide systems, respectively, in this mixed-phase sample.

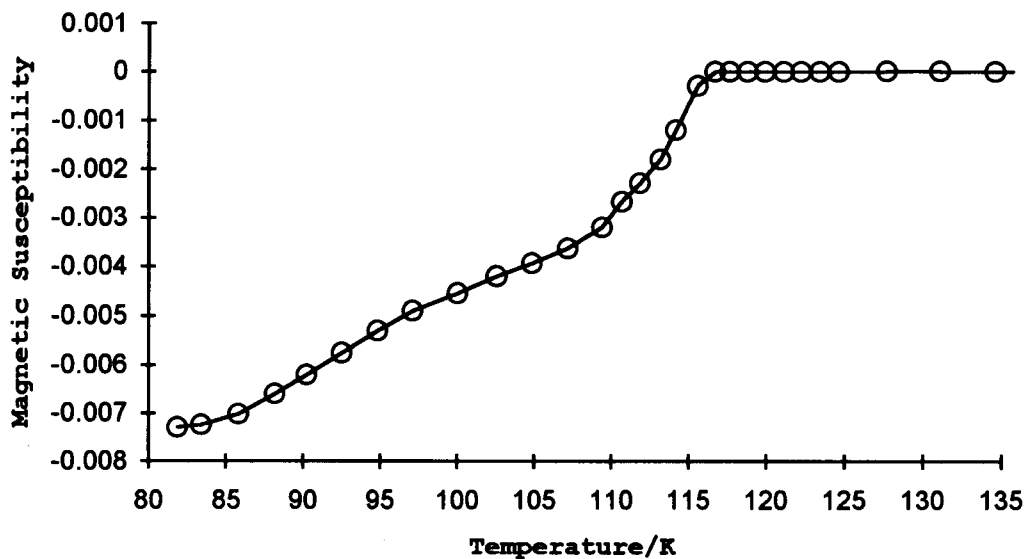


Figure 6. Magnetic susceptibility of  $\text{Tl}_2\text{Ba}_2\text{Ca}_{1.5}\text{Sr}_{0.5}\text{Cu}_3\text{O}_y$ . The  $T_c$  of this sample is 117K. The change in the curvature of the plot around 97K to 105K is evidence for a lower temperature superconducting phase in the sample. The lower temperature superconducting transition is due to the two-layer phase and the 117K superconducting transition is due to the three-layer phase in the sample.

reaction tube without requiring an extra heating step in the preparation process. Soon after using  $\text{SrO}_2$  it was determined that the strontium peroxide yielded better results as a reagent because thallium loss could be minimized. The remainder of the  $\text{Tl}_2\text{Ba}_2\text{Ca}_{1.5}\text{Sr}_{0.5}\text{Cu}_3\text{O}_y$  products made were synthesized using  $\text{SrO}_2$ .

For several samples later attempted at the composition of  $\text{Tl}_2\text{Ba}_2\text{Ca}_{1.5}\text{Sr}_{0.5}\text{Cu}_3\text{O}_y$ , the furnace was adjusted to a set-point temperature from  $875^\circ\text{C}$  to  $925^\circ\text{C}$ , in different experiments, and heated in a time range of four to twelve hours. The samples were heated at the maximum furnace heating rate from room temperature. The time it took to attain the desired set-point temperature at the maximum furnace heating rate averaged about 40 to 50 minutes, depending specifically on the exact parameters (set-point temperature and duration of heating) for a particular experimental run. After the end of the specified heating period, the sample tube was immediately removed from the furnace directly to room temperature.

Powder X-ray diffraction analysis of the products revealed a variety of results for the  $\text{Tl}_2\text{Ba}_2\text{Ca}_{1.5}\text{Sr}_{0.5}\text{Cu}_3\text{O}_y$  experimental attempts. The products that had primarily a three-layer phase were the ones that were subjected to lower synthesis heating temperatures, in the range of  $875^\circ\text{C}$  to  $890^\circ\text{C}$ , and a shorter heating period, typically less than six hours. A set-point temperature of around  $875^\circ\text{C}$  and a heating period of four to five hours produced some of the best results with predominantly three-layer phase products containing very little of the two-layer phase. Figure 7 on page 26 shows a powder X-ray diffraction pattern of a  $\text{Tl}_2\text{Ba}_2\text{Ca}_{1.5}\text{Sr}_{0.5}\text{Cu}_3\text{O}_y$  sample made with  $\text{SrO}_2$ . A greater number of three-layer phase peaks are present in Figure 7 compared to Figure 5.

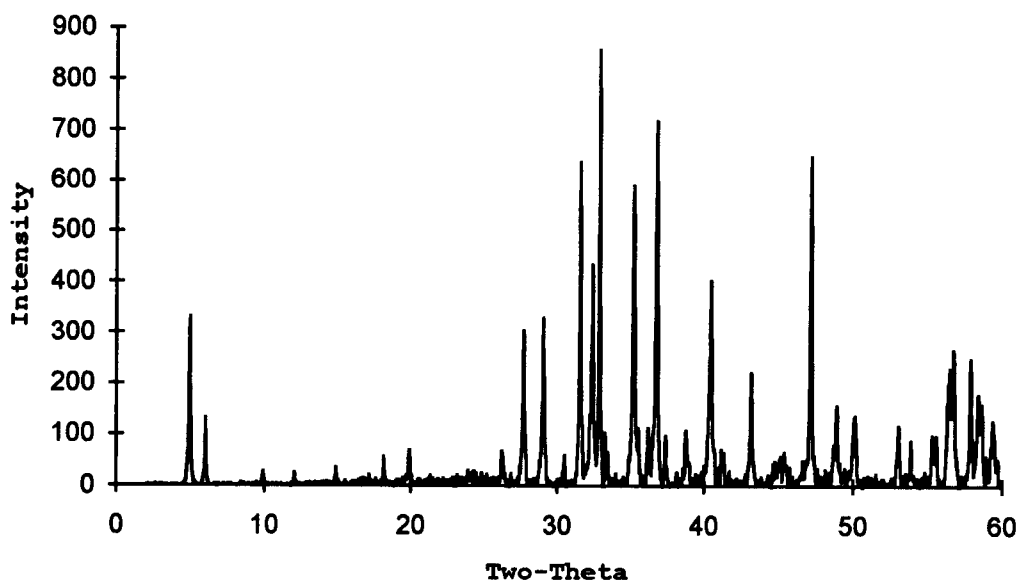


Figure 7. X-ray diffraction pattern #2 of  $\text{Tl}_2\text{Ba}_2\text{Ca}_{1.5}\text{Sr}_{0.5}\text{Cu}_3\text{O}_y$ . This sample was heated four hours at  $875^\circ\text{C}$  in gold tubing.  $\text{SrO}_2$  was used as a reagent. Most of the peaks in the pattern are three-layer phase peaks and a few are two-layer phase peaks. The first sharp peak at  $5^\circ$  two-theta is the three-layer 002 phase peak. The second sharp peak, less intense than the first peak, at  $6^\circ$  two-theta is the two-layer 002 phase peak.

### The $Tl_2Ba_2Ca_{2-x}Sr_xCu_3O_y$ systems

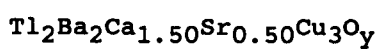
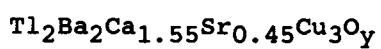
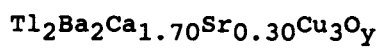
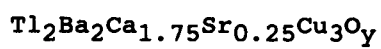
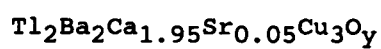
During the same period of time that the  $Tl_2Ba_2Ca_{1.5}Sr_{0.5}Cu_3O_y$  systems were being studied, a series of compounds was attempted with the general formula of  $Tl_2Ba_2Ca_{2-x}Sr_xCu_3O_y$ . Table 1 on page 29 lists the different systems that were investigated.

The reagent oxides were prepared as described in the experimental section. Gold tubes were used for all the samples prepared. The furnace was programmed to heat the  $Tl_2Ba_2Ca_{2-x}Sr_xCu_3O_y$  samples from room temperature to 875°C in 40 minutes. The samples were removed from the furnace to room temperature 20 minutes after the furnace temperature attained 875°C.

The results from X-ray diffraction indicated that all the samples contained mixed phases of the 2212 type structure (based on the two-layer copper oxide  $Tl_2Ba_2CaCu_2O_8$  structure) and the 2223 three-layer copper oxide structure. There were no trends seen in the results to relate the level of strontium doping to the small differences seen in the powder X-ray diffraction data. Every product had results of two-layer and three-layer phases, as evidenced from X-ray diffraction data. Many of the X-ray diffraction patterns showed very weak two-layer and three-layer peak intensities relative to the intensities of the higher two-theta angle peaks. Figure 8 on page 30 shows a typical X-ray powder diffraction pattern seen in this series.

Of the several attempts at synthesizing the  $Tl_2Ba_2Ca_{2-x}Sr_xCu_3O_y$  samples using the gold tubing containers, about one-half of all the sample tubes remained sealed throughout the furnace heating program. These reactions were done before silica tubing was employed to monitor

thallium leakage from reaction tubes, therefore it was not known if any of the apparently sealed tubes actually remained hermetically-sealed throughout these experiments.

Table 1. The  $\text{Tl}_2\text{Ba}_2\text{Ca}_{2-x}\text{Sr}_x\text{Cu}_3\text{O}_y$  series.

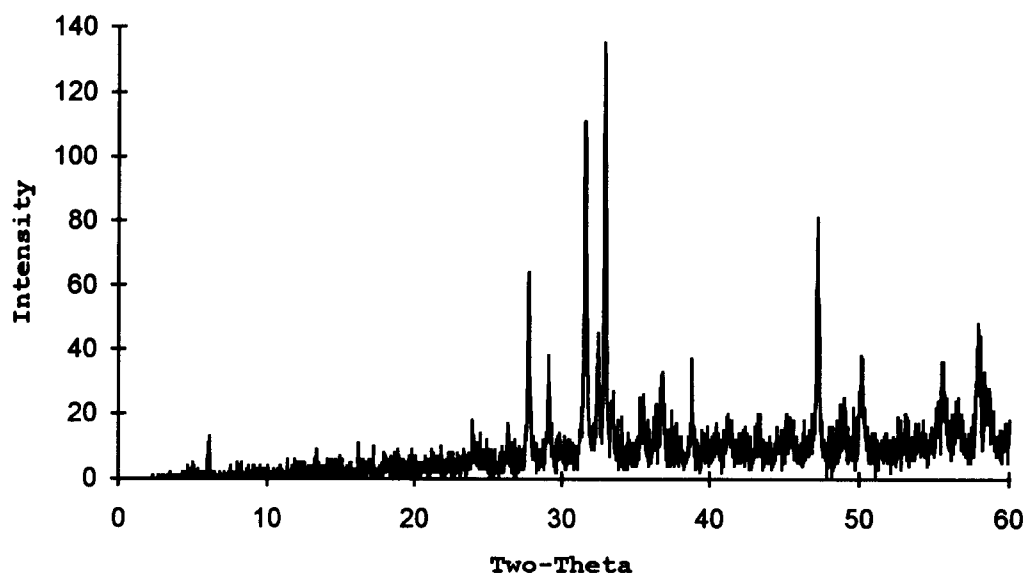


Figure 8. X-ray diffraction pattern of  $\text{Tl}_2\text{Ba}_2\text{Ca}_{1.85}\text{Sr}_{0.15}\text{Cu}_3\text{O}_y$ . A small and broad peak around  $5^\circ$  and a larger and sharp peak around  $6^\circ$  two-theta show the three-layer and two-layer phases present in this sample. The two-layer and three-layer 002 peaks had relatively weak intensities in the  $\text{Tl}_2\text{Ba}_2\text{Ca}_{2-x}\text{Sr}_x\text{Cu}_3\text{O}_y$  products.

### The $Tl_2Ba_2Ca_3Cu_4O_{12}$ and $Tl_2Ba_2Ca_{3-x}Sr_xCu_4O_y$ systems

Increasing the heating time or temperature, or both, are two methods to have greater, if not complete, formation of a single-phase three-layer product. Another method is to adjust the reagent stoichiometries of the reactants that can help define and form the desired three-layer phase. The general stoichiometry of  $Tl_2Ba_2Ca_{3-x}Sr_xCu_4O_y$  has increased calcium oxide and copper oxide ratios in the starting composition as compared with the previously discussed  $Tl_2Ba_2Ca_{2-x}Sr_xCu_3O_y$  formula.

Several attempts at synthesizing three-layer phases using a starting composition of four-layer stoichiometry were found to be successful when shorter furnace heating times were used. The formula of  $Tl_2Ba_2Ca_3Cu_4O_{12}$  is an example of a four-layer copper oxide structure that has a reported  $T_c$  of 119K.<sup>22</sup> The aim was to use a stoichiometric excess of some of the reagents (primarily calcium oxide and copper oxide) and to heat the reagents long enough to form the three-layer phase in the product, but stop the heating before any significant four-layer phase formation takes place.

The products that formed from the starting reagent stoichiometry of  $Tl_2Ba_2Ca_3Cu_4O_{12}$  had very promising results indicating three-layer phase formation when heated for 90 minutes at 875°C in sealed gold tubing. Figure 9 on page 33 shows a powder X-ray diffraction pattern of one stoichiometric four-layer system that actually produced a three-layer phase in the bulk of the product along with a portion of a two-layer phase. The figure shows the 002 peak of the three-layer phase to be sharp and intense whereas the 002 peak of the two-layer phase is

absent. The lowest observed two-layer phase peak in the figure is the 004 peak around  $13^\circ$  two-theta. Most of the peaks in the X-ray diffraction pattern of Figure 9 are three-layer phase peaks, and relatively fewer of the peaks are of the two-layer phase.

Silver tubes were first employed for experimental work with some of the  $\text{Tl}_2\text{Ba}_2\text{Ca}_{3-x}\text{Sr}_x\text{Cu}_4\text{O}_y$  systems. Further experiments performed with the  $\text{Tl}_2\text{Ba}_2(\text{Ca}_{0.85}\text{Sr}_{0.15})_{x-1}\text{Cu}_x\text{O}_y$  systems, during the same time research with the  $\text{Tl}_2\text{Ba}_2\text{Ca}_{3-x}\text{Sr}_x\text{Cu}_4\text{O}_y$  systems were performed, indicated that silver tubing could be used as effectively as gold tubing at temperatures up to  $875^\circ\text{C}$  for sustained heating periods of up to four or five hours.

Relatively few  $\text{Tl}_2\text{Ba}_2(\text{Ca}_{0.85}\text{Sr}_{0.15})_{x-1}\text{Cu}_x\text{O}_y$  systems were synthesized in the study. The X-ray diffraction data results indicated that most of these systems formed two-layer and three-layer phase products. The X-ray diffraction data for the products of these systems were similar to the mixed-phase X-ray diffraction data seen in the previous studies of the  $\text{Tl}_2\text{Ba}_2\text{Ca}_{1.5}\text{Sr}_{0.5}\text{Cu}_3\text{O}_y$  and the  $\text{Tl}_2\text{Ba}_2\text{Ca}_{2-x}\text{Sr}_x\text{Cu}_3\text{O}_y$  systems. The important results from the studies of the  $\text{Tl}_2\text{Ba}_2(\text{Ca}_{0.85}\text{Sr}_{0.15})_{x-1}\text{Cu}_x\text{O}_y$  systems indicated that silver tubing could be effectively used as a reaction container.

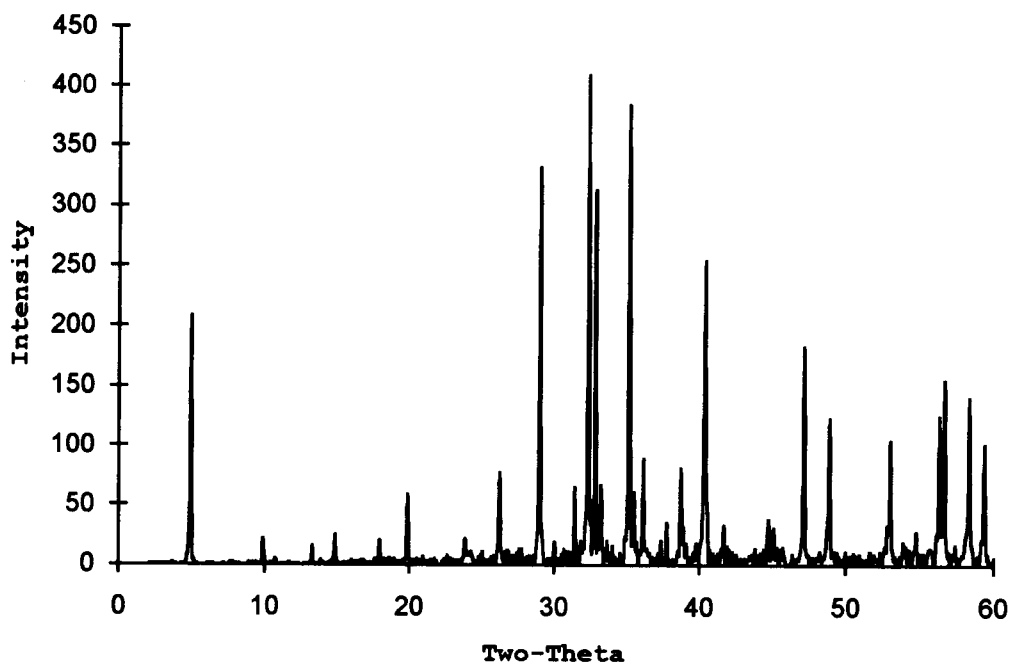


Figure 9. X-ray diffraction pattern of  $\text{Tl}_2\text{Ba}_2\text{Ca}_3\text{Cu}_4\text{O}_{12}$ . Most of the peaks in this pattern correspond to the formation of a three-layer phase product. This sample was heated for 90 minutes at  $875^\circ\text{C}$  in a sealed gold tube. This sample was one of the first synthesized in this study with a stoichiometric excess of the calcium oxide and copper oxide reagents.

Table 2 on page 36 shows some compounds that were heated in both silver and gold tubing in the  $Tl_2Ba_2(Ca_{0.85}Sr_{0.15})_{x-1}Cu_xO_y$  series where  $x$  ranged from 3.5 to 3.8. The  $T_c$ 's for the range of products in these systems were also measured and are listed in Table 2.

Several experiments in the  $Tl_2Ba_2Ca_{3-x}Sr_xCu_4O_y$  system were explored with different levels of strontium substitution. Table 3 on page 37 lists the stoichiometries attempted.

The reagents were heated from room temperature to  $875^\circ C$  for a total time of at least 90 minutes and no longer than four hours with silver container tubing. Experiments attempted with heating times of less than 90 minutes had incomplete single-phase three-layer formation, as evidenced by two-layer phase formation. Further experiments to heat the samples in silver tubing for longer than four hours often caused sample container leakage due to hole formation, cracks, tube fatigue, or collapse.

The majority of the samples prepared in the  $Tl_2Ba_2Ca_{3-x}Sr_xCu_4O_y$  systems were heated between two and four hours. At the end of a given furnace heating period, the samples were immediately removed from the furnace to room temperature. Compounds synthesized with the starting compositions of  $x = 0.05, 0.10, 0.15, 0.25,$  and  $0.50,$  had products of mixed phases, mostly the two-layer and three-layer copper oxide products for heating times of around two hours. The samples heated for about three hours at  $875^\circ C$  gave good results with mostly three-layer phases present in the product and relatively few occurrences of sample tube opening during the furnace heating period. Samples heated for as long as four hours at  $875^\circ C$  often did not give good results due to sample tube opening.

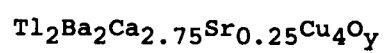
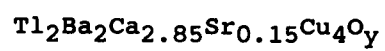
In many of the products of the  $\text{Tl}_2\text{Ba}_2\text{Ca}_{3-x}\text{Sr}_x\text{Cu}_4\text{O}_y$  series, the three-layer phase 002 peak, seen in X-ray diffraction data, was much more prominent when compared with the two-layer phase 002 peak. Variably, the 002 peak and other low-angle peaks of the two-layer phase were absent in many of the  $\text{Tl}_2\text{Ba}_2\text{Ca}_{3-x}\text{Sr}_x\text{Cu}_4\text{O}_y$  samples. However, the presence or absence of the two-layer phase peaks was not predictable and did not correlate with the level of strontium substitution.

Table 2. Products of the  $Tl_2Ba_2(Ca_{0.85}Sr_{0.15})_{x-1}Cu_xO_y$  series. All the samples were heated from room temperature to  $875^\circ C$  and allowed to heat for the time specified. The samples were removed directly to room temperature at the end of the heating period.

---

Tube type	x	Heating time	$T_c$ (K)
Ag	3.8	4 hrs.	114
Au	3.8	4 hrs.	113
Ag	3.7	4 hrs.	111
Au	3.7	4 hrs.	110
Ag	3.6	4 hrs.	112
Au	3.6	4 hrs.	112
Ag	3.5	4 hrs.	113
Au	3.5	4 hrs.	112
Ag	3.75	4 hrs.	115
Au	3.75	3 hrs.	111
Ag	3.65	4 hrs.	115
Au	3.65	3 hrs.	113
Ag	3.55	4 hrs.	114
Au	3.55	3 hrs.	108
Ag	3.8	2 hrs.	111
Au	3.8	2 hrs.	107
Ag	3.7	2 hrs.	107
Au	3.7	2 hrs.	107
Ag	3.6	2 hrs.	106
Au	3.6	2 hrs.	105
Ag	3.5	2 hrs.	108
Au	3.5	2 hrs.	107

---

Table 3. The  $\text{Tl}_2\text{Ba}_2\text{Ca}_{3-x}\text{Sr}_x\text{Cu}_4\text{O}_y$  series.

Of the sets of products made in the  $Tl_2Ba_2Ca_{3-x}Sr_xCu_4O_y$  series, the  $Tl_2Ba_2Ca_{2.85}Sr_{0.15}Cu_4O_y$  product indicated the best results for single-phase three-layer formation when heated at 870-875°C in the time range of three to three-and-a-half hours. The X-ray diffraction pattern, seen in Figure 10 on page 39, has a relatively strong 002 low-angle peak at 5° two-theta, indicating the formation of a three-layer phase in the product. The other three-layer phase peaks of the 004, 006, and 008 phases are also visibly present and provide further evidence for the formation of the three-layer phase in the product. The magnetic susceptibility data for this sample shows a three-layer phase transition of 112K in Figure 11 (on page 40).

Only a few  $Tl_2Ba_2Ca_{2.85}Sr_{0.15}Cu_4O_y$  products out of many experimental attempts could be made with reproducible  $T_c$ 's and X-ray diffraction patterns with preparation and synthesis of samples under the same conditions. X-ray diffraction patterns for other  $Tl_2Ba_2Ca_{2.85}Sr_{0.15}Cu_4O_y$  systems indicated mixing of the two-layer phase with the three-layer phase in the products. The  $T_c$ 's measured for the products synthesized with the  $Tl_2Ba_2Ca_{2.85}Sr_{0.15}Cu_4O_y$  stoichiometry ranged from 104K to 112K. The factor that contributed greatly to the broad range of  $T_c$ 's and often mixed-phase X-ray diffraction data was the failure of the sealed reaction tubes during the furnace heating period.

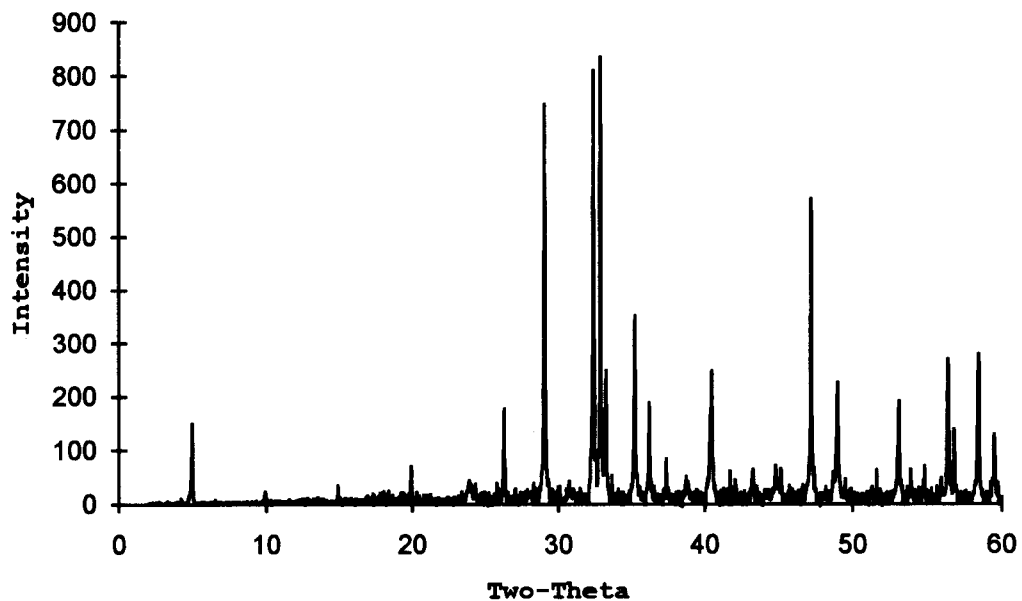


Figure 10. X-ray diffraction pattern of  $\text{Tl}_2\text{Ba}_2\text{Ca}_{2.85}\text{Sr}_{0.15}\text{Cu}_4\text{O}_y$ . This product has definite three-layer phase peaks at the 002, 004, 006, and 008 peak reflections located at approximately  $5^\circ$ ,  $10^\circ$ ,  $15^\circ$ , and  $20^\circ$  two-theta.

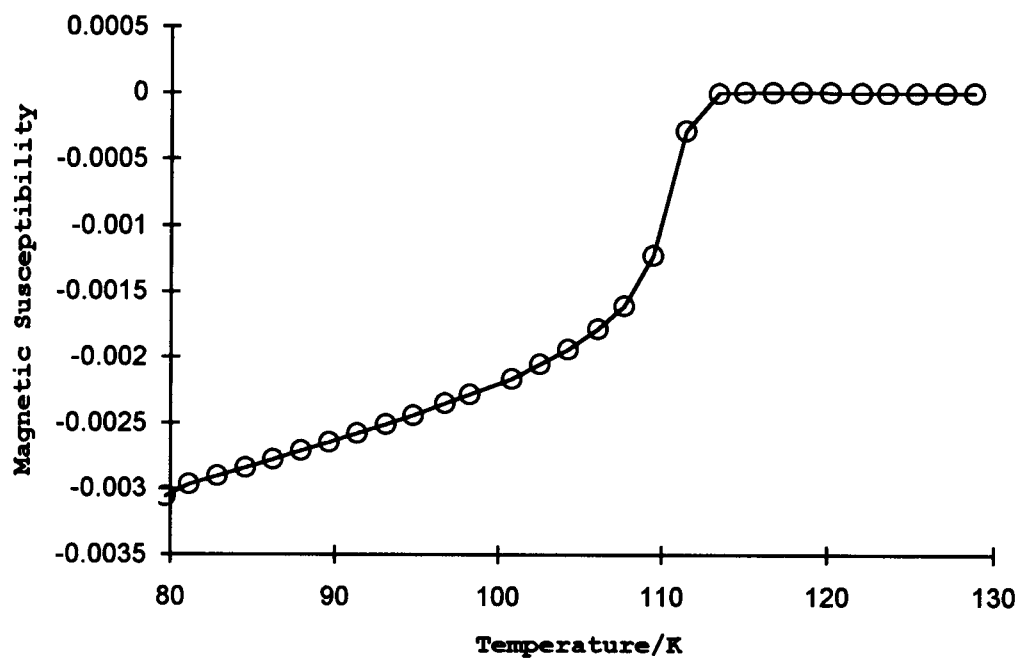


Figure 11. Magnetic susceptibility of  $\text{Tl}_2\text{Ba}_2\text{Ca}_{2.85}\text{Sr}_{0.15}\text{Cu}_4\text{O}_y$ . The  $T_c$  of this product is 112K.

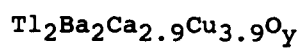
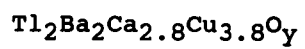
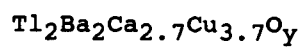
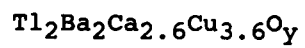
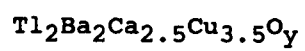
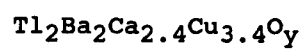
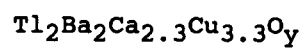
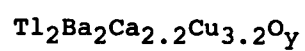
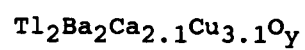
### The $Tl_2Ba_2Ca_{2+x}Cu_{3+x}O_y$ systems

Results from the  $Tl_2Ba_2Ca_{2-x}Sr_xCu_3O_y$  systems and the  $Tl_2Ba_2Ca_{3-x}Sr_xCu_4O_y$  systems suggested that an ideal three-layer phase product might have a stoichiometry in the range somewhere between the two sets of systems. A variety of synthesis conditions had already been attempted for the various systems, which produced a range of results. Therefore, a new set of experiments were planned to establish what other synthesis conditions could be used with the silver tube containers. Gold tube containers were no longer being used at this point in the study.

To determine optimized temperature programs, starting compositions, and reaction conditions for strontium-substituted products, it proved beneficial to take a step back and first determine the best sample preparatory steps, conditions, and parameters for the non-strontium-substituted products. Experiments to synthesize the non-strontium-substituted 2223 were performed to find out the most ideal reactant stoichiometries, heating times, parameters, and conditions that might be used for the strontium-substituted system syntheses.

Various compounds with the general stoichiometry of  $Tl_2Ba_2Ca_{2+x}Cu_{3+x}O_y$  were prepared. The values of  $x$  ranged from 0.1 to 0.9 in several different experiments. Table 4 on page 42 lists a range of stoichiometries that were experimentally explored in an attempt to find single-phase three-layer products in the  $Tl_2Ba_2Ca_{2+x}Cu_{3+x}O_y$  systems.

All the products in the  $Tl_2Ba_2Ca_{2+x}Cu_{3+x}O_y$  series were synthesized in sealed silver tubing. Heating parameters were varied for several

Table 4. The  $\text{Tl}_2\text{Ba}_2\text{Ca}_{2+x}\text{Cu}_{3+x}\text{O}_y$  series.

different starting stoichiometries with temperatures from 850°C to 875°C and heating times from 90 minutes to four hours. The compound with the starting composition of  $Tl_2Ba_2Ca_{2.5}Cu_{3.5}O_y$  had the best results to indicate the formation of a three-layer phase in the product with very few impurities and mixed phases. Figure 12 on page 44 represents one of the best powder X-ray diffraction patterns observed for a  $Tl_2Ba_2Ca_{2.5}Cu_{3.5}O_y$  product.

The synthesis conditions that resulted in the formation of the  $Tl_2Ba_2Ca_{2.5}Cu_{3.5}O_y$  product were heating the sample in a sealed silver tube from room temperature to the dwell temperature of 865°C at the maximum ramp rate of the furnace. A dwell temperature of 865°C was typically reached by the furnace in about 45 minutes when starting from room temperature. The sample remained in the furnace for four hours through the dwell period and then later was removed directly to room temperature. This compound showed a relatively sharp transition curve in the magnetic susceptibility data. The measured  $T_C$ 's of some of the best  $Tl_2Ba_2Ca_{2.5}Cu_{3.5}O_y$  products were as high as 115K, as one example is shown in Figure 13 (page 45).

Inspection of the sample container tubes, that contained most of the sample products of the  $Tl_2Ba_2Ca_{2.5}Cu_{3.5}O_y$  systems, very soon after the heating showed that most of the tubes had no visibly apparent reagent or product leakage. Most of the tubes remained sealed throughout the entire furnace heating program. The experimental results were not readily reproduced as no two runs ever revealed identical  $T_C$  curves, nor identical X-ray diffraction patterns.

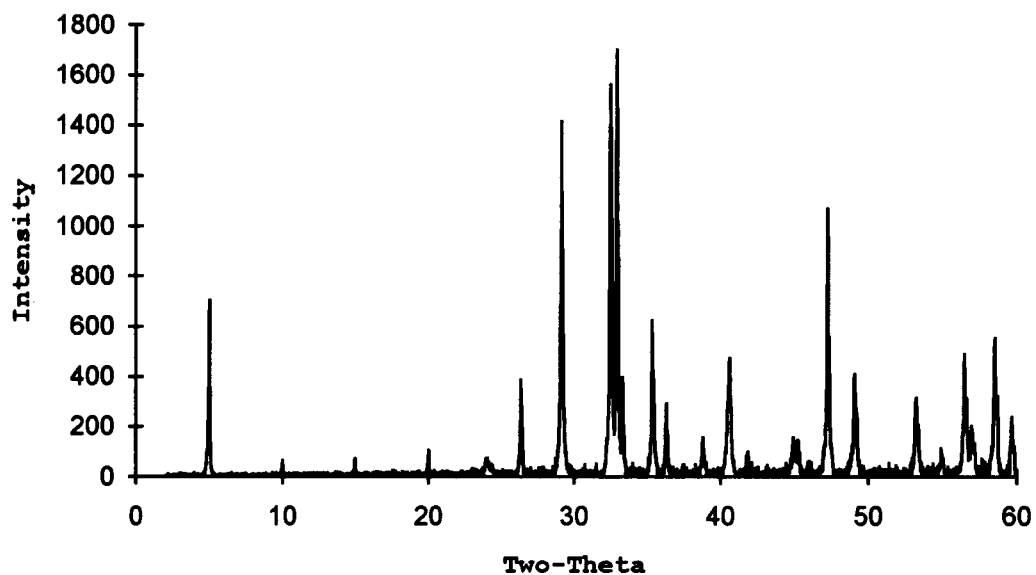


Figure 12. X-ray diffraction pattern of  $\text{Tl}_2\text{Ba}_2\text{Ca}_{2.5}\text{Cu}_{3.5}\text{O}_y$ . This compound shows strong three-layer peaks at the 002, 004, 006, and 008 lines located at approximately  $5^\circ$ ,  $10^\circ$ ,  $15^\circ$ , and  $20^\circ$  two-theta.

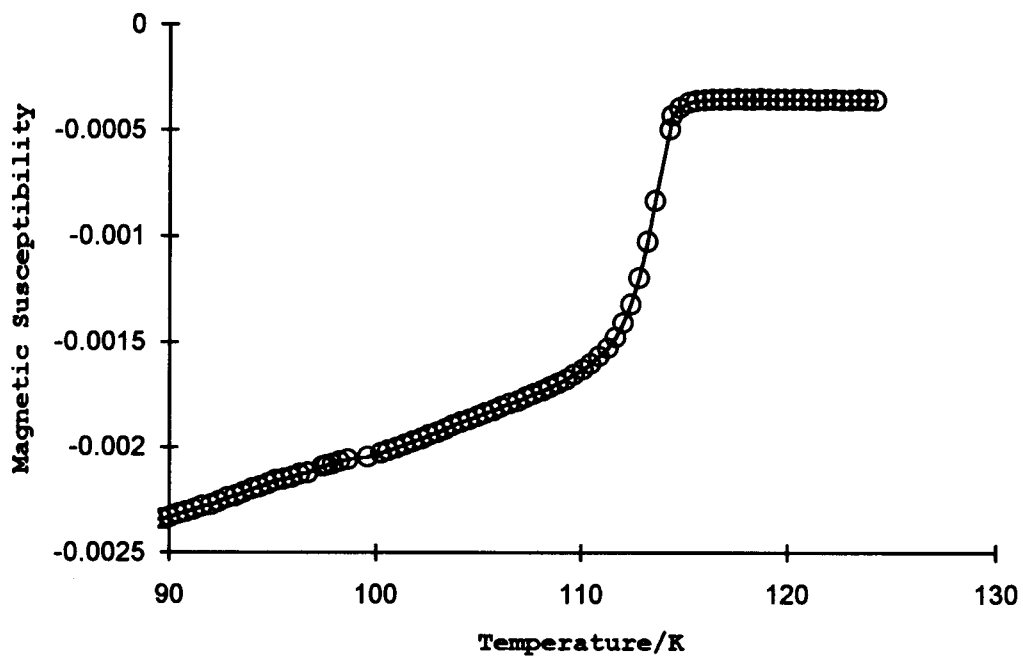


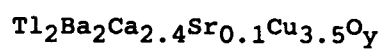
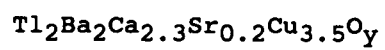
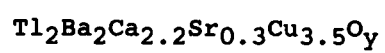
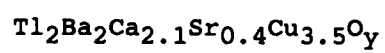
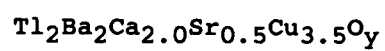
Figure 13. Magnetic susceptibility of  $\text{Tl}_2\text{Ba}_2\text{Ca}_{2.5}\text{Cu}_{3.5}\text{O}_y$ . The  $T_C$  of this product is 115K.

### The $Tl_2Ba_2Ca_{2.5-x}Sr_xCu_{3.5}O_y$ systems

With some successful results in synthesizing near-single-phase three-layer products in the  $Tl_2Ba_2Ca_{2+x}Cu_{3+x}O_y$  system, where  $x = 0.5$ , further experiments were planned to attempt to substitute strontium for calcium in different amounts. Using the formula of  $Tl_2Ba_2Ca_{2.5}Cu_{3.5}O_y$  as a parent compound, strontium was substituted stoichiometrically in for calcium. The research started with the formula of  $Tl_2Ba_2Ca_{2.5-x}Sr_xCu_{3.5}O_y$ , where strontium was substituted in the range of  $x = 0.1$  to  $0.5$ . Table 5 on page 47 lists the  $Tl_2Ba_2Ca_{2.5-x}Sr_xCu_{3.5}O_y$  systems that were investigated.

The strontium-substituted samples were, in every case, heated in the same furnace at the same time and under the same temperature conditions for each batch or series of samples. For example,  $Tl_2Ba_2Ca_{2.4}Sr_{0.1}Cu_{3.5}O_y$  and the other four samples where strontium was stoichiometrically incremented by 0.1 and calcium was stoichiometrically decremented by 0.1, were prepared and sealed at the same time in individual silver tubing containers of similar size. All the samples were placed together for a simultaneous heating in the same furnace. This method was the best way to keep uniformity of the conditions and parameters to which the samples of the series were subjected.

After heating many of the  $Tl_2Ba_2Ca_{2.5-x}Sr_xCu_{3.5}O_y$  samples it was noted on several occasions that there were more occurrences of reagent loss and leakage from the silver tubing containers, at some point during the heating, when compared with the  $Tl_2Ba_2Ca_{2+x}Cu_{3+x}O_y$  samples. A few samples with strontium had no tube leakage problem, whereas many others unpredictably had some tube leakage, and to varying degrees.

Table 5. The  $\text{Tl}_2\text{Ba}_2\text{Ca}_{2.5-x}\text{Sr}_x\text{Cu}_3.5\text{O}_y$  series.

Open-ended silica tubes were used to qualitatively monitor for thallium leakage from the silver tube containers during the heating time in the furnace. The silver tube containers that appeared to have no visible holes or leakage (from visual inspection) variably and often did leak (thallium) reagent vapors during the furnace heating period. Silica tubing works well to detect thallium leakage because silica easily reacts with thallium at high temperatures. The silver tube containers often did have vapor leakage from the ends of the tubes, primarily where the crimps had been melted shut. Evidence of the (thallium) reagent vapor leakage was seen on the silica tubing in the near vicinity of the silver tubing container crimps.

Modified heating profiles for the strontium-substituted samples that had not been previously attempted for the non-strontium-substituted samples were tried. This modified approach required pre-heating the furnace, without any samples, to a dwell temperature of 865°C, then inserting the silver tube containers with samples (within supporting silica tubes) into the furnace for a specific amount of time, and later removing the silver tube containers to room temperature. Heating times of approximately two, four, and six hours were attempted at the dwell temperature of 865°C. The experiments were planned to see if any trends existed between the amount of strontium substitution and the successful formation of a single-phase compound. The trends of  $T_c$  versus level of strontium substitution were also under investigation in these experiments.

The experiments were performed such that three different sets of silver tube containers, sealed with reagents of the same stoichiometry, were put into the same furnace for two, four, and six hours. At the end

of each two-hour heating period, one set of sample tube containers were removed. Therefore, the first set of tubes were removed after two hours of heating, the second set of tubes were removed after four hours of heating, and the last set of tubes were removed after six hours of heating.

Of the experiments that were conducted as described above, only a couple of the experiments had results where there was little or no reagent leakage from all the silver tube containers heated for the different periods of time. Most of the experiments had results where some tubes opened up considerably more than other tubes when heated for similar time periods. Much the data from these experiments were discounted because no measure of reproducibility could be established from experiment to experiment. Table 6 on page 50 summarizes the measured  $T_C$  data from the best experiment where reagent loss was minimal, though not necessarily equal, for all the silver tube containers. Some of the highest measured  $T_C$ 's, up to 117K, in this study were seen in the  $Tl_2Ba_2Ca_{2.5-x}Sr_xCu_{3.5}O_y$  systems where the method of quick heating and quick cooling were used.

Table 6.  $Tl_2Ba_2Ca_{2.5-x}Sr_xCu_{3.5}O_y$  heating time and  $T_c$  data. All samples were heated at  $865^\circ C$  for the specified time listed in the table.  $T_c$ 's were measured for samples heated for 2, 4, and 6 hours.

Product	$T_c$ @ 2 hrs.	$T_c$ @ 4 hrs.	$T_c$ @ 6 hrs.
$Tl_2Ba_2Ca_{2.4}Sr_{0.1}Cu_{3.5}O_y$	114K	NSC <sup>a</sup>	116K
$Tl_2Ba_2Ca_{2.3}Sr_{0.2}Cu_{3.5}O_y$	115K	116K	NSC <sup>a</sup>
$Tl_2Ba_2Ca_{2.2}Sr_{0.3}Cu_{3.5}O_y$	112K	117K	117K
$Tl_2Ba_2Ca_{2.1}Sr_{0.4}Cu_{3.5}O_y$	114K	114K	117K
$Tl_2Ba_2Ca_{2.0}Sr_{0.5}Cu_{3.5}O_y$	114K	116K	116K

<sup>a</sup> denotes the marked product is non-superconducting (to 90K).

### Post-synthesis annealing treatment

Post-annealing experiments were attempted with some products to see if the measured  $T_C$  could be increased following annealing treatment. The powder samples prepared for annealing were put in an open alumina boat and the boat was placed into a tube furnace. Safe  $H_2(g)$  ( $H_2(g)$  diluted with argon gas) or  $N_2(g)$  was used for reducing conditions and  $O_2(g)$  was used for oxidizing conditions. Typical annealing temperatures were in the range of  $300^\circ C$  to  $400^\circ C$  for a time period of one to six hours. While the samples were annealing in the tube furnace, they were always in the flow of the annealing gas, which usually was set to a flowrate of a few milliliters per second.

A few experiments were performed to anneal  $Tl_2Ba_2Ca_{1.5}Sr_{0.5}Cu_3O_y$  samples with safe  $H_2(g)$ . Annealing temperatures between  $300^\circ C$  and  $350^\circ C$  were attempted from one hour to six hours. Powder samples annealed for less than three hours at temperatures around  $300^\circ C$  showed no change in the powder appearance or color, peak profiles in the X-ray diffraction pattern, nor the  $T_C$  in magnetic susceptibility measurements. The samples remained as a black powder just as they were before the annealing treatment.

In other experiments, increasing either the annealing temperature or the duration of the annealing time invariably resulted in powder products that were blackish-brown to brown. Powder X-ray diffraction data showed that any three-layer phases that were present in the sample before the annealing treatment became absent after the annealing treatment. Figure 14 on page 53 shows an X-ray diffraction pattern of a  $Tl_2Ba_2Ca_{1.5}Sr_{0.5}Cu_3O_y$  sample that has no low angle 002, 004, 006, or 008

peaks, thus suggesting the absence of the three-layer (and also the two-layer) phase in the annealed product. The X-ray diffraction pattern in Figure 14 is very typical of many other X-ray diffraction patterns of samples from other systems where annealing treatment was attempted.

In general, all samples that were normally superconducting before any annealing treatment became non-superconducting (measured to 77K) as annealing temperatures were raised or annealing times were increased. Further annealing experiments using  $N_2(g)$  for reducing conditions and  $O_2(g)$  for oxidizing conditions did not result in any significant differences for several other studied systems. In essentially all cases of the annealing studies, there were no observed changes in the X-ray diffraction and magnetic susceptibility data nor were there any significant changes that enhanced the superconducting structural phase and measured  $T_C$ .

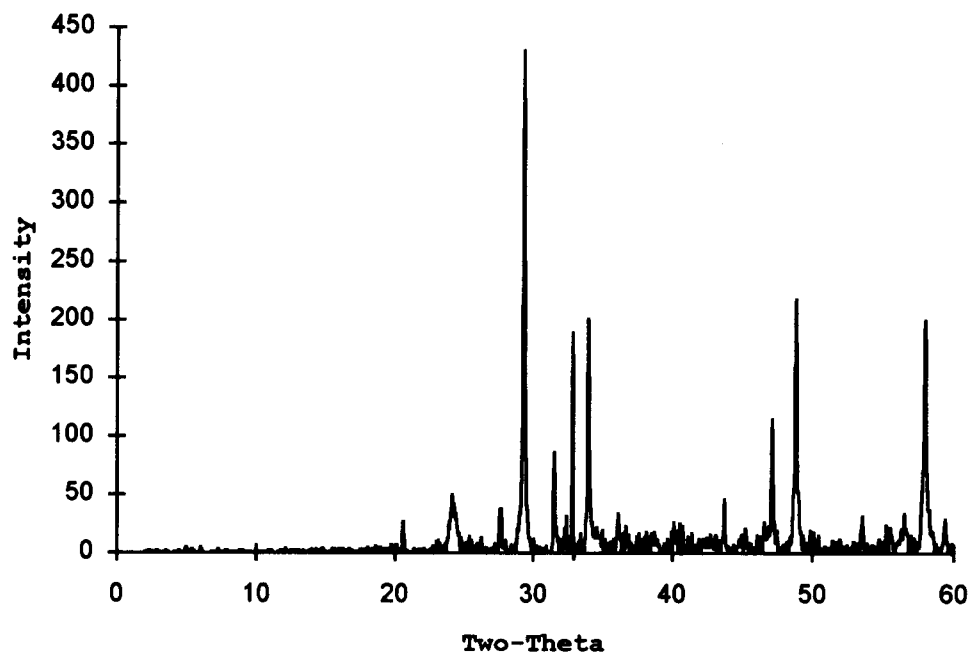


Figure 14. Annealed  $\text{Tl}_2\text{Ba}_2\text{Ca}_{1.5}\text{Sr}_{0.5}\text{Cu}_3\text{O}_y$  X-ray pattern. This X-ray diffraction pattern is very typical for all the samples that were either annealed for more than three hours or at temperatures close to  $400^\circ\text{C}$ , or both. This particular sample that had a pre-annealed  $T_c$  of 116K became non-superconducting after annealing under reducing conditions with safe  $\text{H}_2(\text{g})$  for 6 hours at  $350^\circ\text{C}$ .

### Least-Squares Cell Refinement

Least-squares cell refinement calculations were done for some of the studied systems where good X-ray diffraction results could be used with an internal silicon standard to determine unit cell dimensions. The systems chosen for refinement calculations were ones that had essentially single-phase three-layer products. Single-phase products were important for accuracy in cell dimension refinement determinations. Almost any amount of a phase other than the three-layer copper oxide phase, such as the two-layer copper oxide phase, could show up as stray or false three-layer peaks in X-ray diffraction patterns (primarily at the higher two-theta angles) when doing single-phase cell dimension refinement. Incorrect peaks used for single-phase cell refinement calculations can give rise to very misleading and erroneous refinement results. Because it was imperative that the correct phase peaks be used in refinement calculations, the amount of samples that could be considered for valid least-squares cell refinement were severely limited.

As mentioned in the introduction, the  $\text{Tl}_2\text{Ba}_2\text{Ca}_2\text{Cu}_3\text{O}_{10}$  structure is tetragonal with an *a*-axis cell length of 3.85 Å and a *c*-axis cell length of 35.88 Å.<sup>8</sup> The other phases in the system of  $\text{Tl}_2\text{Ba}_2\text{Ca}_{n-1}\text{Cu}_n\text{O}_{2n+4}$  differ primarily in the *c*-axis cell dimension and not in the *a*-axis cell dimension. The *a*-axis cell dimension is invariably in the range of 3.85 Å to 3.87 Å for the one, two, and three-layer phases of the  $\text{Tl}_2\text{Ba}_2\text{Ca}_{n-1}\text{Cu}_n\text{O}_{2n+4}$  system. The *c*-axis cell dimension can range from 23.24 Å for the one-layer copper oxide structure to 35.88 Å for the three-layer copper oxide structure.<sup>8,12,13</sup>

Therefore, due to the greater length of the  $c$ -axis cell dimension in the  $Tl_2Ba_2Ca_{n-1}Cu_nO_{2n+4}$  tetragonal systems, the variations of the  $c$ -axis cell lengths in cell refinement calculations, especially with respect to strontium substitution, were of primary interest.

The  $Tl_2Ba_2Ca_{2+x}Cu_{3+x}O_y$  system was refined for the single-phase three-layer products seen in the range where  $x = 0.4$  to  $0.8$ . Table 7 on page 57 lists the products and the refined  $c$ -axis cell dimensions.

Refinement was also done for the  $Tl_2Ba_2Ca_{2.5-x}Sr_xCu_{3.5}O_y$  systems where predominantly single-phase three-layer products formed. The  $T_c$ 's had been previously measured and were reported in Table 6 (page 50). Table 8 on page 58 lists the products, synthesis conditions, and refined  $c$ -axis cell dimensions for these systems synthesized in silver tube containers.

The  $c$ -axis least-squares cell refinement data in Tables 7 and 8 are not statistically significant in order to make any correlation between sample stoichiometry and  $c$ -axis cell length. In the case of the products listed in Table 7, the calcium oxide and copper oxide levels were incremented in successive samples, however, no trend was seen in the refined  $c$ -axis cell dimension. More importantly, the standard deviation is large for each refinement, thus rendering the refinement data statistically insignificant.

Table 8 lists a set of five samples that were heated for time periods of two, four, and six hours at  $865^\circ\text{C}$ . Strontium was substituted in increasing amounts, however, the unit-cell refinement data showed no trends correlating the level of strontium substitution and  $c$ -axis cell lengths. Nonetheless, all the refinement data for these systems are also statistically insignificant because of the very large standard

deviations calculated in most of the refinements, with some standard deviation values approaching 1.5 Å.

Table 7.  $\text{Tl}_2\text{Ba}_2\text{Ca}_{2+x}\text{Cu}_{3+x}\text{O}_y$  refined *c*-axis cell dimensions.

Product	<i>c</i> -axis length (Å)	<i>c</i> -axis standard deviation (Å)
$\text{Tl}_2\text{Ba}_2\text{Ca}_{2.4}\text{Cu}_{3.4}\text{O}_y$	35.73	0.37
$\text{Tl}_2\text{Ba}_2\text{Ca}_{2.5}\text{Cu}_{3.5}\text{O}_y$	35.68	0.40
$\text{Tl}_2\text{Ba}_2\text{Ca}_{2.6}\text{Cu}_{3.6}\text{O}_y$	35.71	0.24
$\text{Tl}_2\text{Ba}_2\text{Ca}_{2.7}\text{Cu}_{3.7}\text{O}_y$	35.71	0.41
$\text{Tl}_2\text{Ba}_2\text{Ca}_{2.8}\text{Cu}_{3.8}\text{O}_y$	35.79	0.71

Table 8.  $Tl_2Ba_2Ca_{2.5-x}Sr_xCu_{3.5}O_y$  refined *c*-axis cell dimensions. All the products were heated at 865°C for the time specified in the table. The standard deviation of the *c*-axis cell dimension is listed in parentheses below its respective refined *c*-axis cell dimension.

Product	Heating Time		
	2 hrs.	4 hrs.	6 hrs.
	<i>c</i> -axis cell dimension (Å)		
$Tl_2Ba_2Ca_{2.4}Sr_{0.1}Cu_{3.5}O_y$	35.70 (0.38)	35.44 (0.74)	36.92 (1.01)
$Tl_2Ba_2Ca_{2.3}Sr_{0.2}Cu_{3.5}O_y$	35.66 (0.53)	36.03 (0.63)	35.04 (0.94)
$Tl_2Ba_2Ca_{2.2}Sr_{0.3}Cu_{3.5}O_y$	35.65 (0.60)	35.77 (0.51)	35.83 (0.87)
$Tl_2Ba_2Ca_{2.1}Sr_{0.4}Cu_{3.5}O_y$	35.71 (0.66)	35.85 (0.91)	35.80 (1.18)
$Tl_2Ba_2Ca_{2.0}Sr_{0.5}Cu_{3.5}O_y$	35.69 (1.47)	35.55 (0.87)	35.69 (1.21)

## SUMMARY AND CONCLUSIONS

$Tl_2Ba_2Ca_{1.5}Sr_{0.5}Cu_3O_y$ , the first system of this study, was synthesized by a non-hermetic pre-heating step to drive away as much  $CO_2(g)$  from the  $SrCO_3$  reagent as possible. This method of pre-heating the reagents yielded unsatisfactory results because many products of two-layer and three-layer mixed-phases were being formed due to the thallium reagent loss in the non-hermetically sealed sample tube heating. Experiments performed with  $SrO_2$  as a reagent indicated that less thallium reagent was lost by hermetically sealing the sample tubes. As a consequence, a greater number of experiments resulted in three-layer phase products.  $T_c$ 's up to 117K were observed in a few  $Tl_2Ba_2Ca_{1.5}Sr_{0.5}Cu_3O_y$  products.

The  $Tl_2Ba_2Ca_{2-x}Sr_xCu_3O_y$  series was explored at the same time with the  $Tl_2Ba_2Ca_{1.5}Sr_{0.5}Cu_3O_y$  system to determine better sample stoichiometries and synthesis parameters. The  $Tl_2Ba_2Ca_{2-x}Sr_xCu_3O_y$  series experiments resulted in all mixed-phase two-layer and three-layer products, mainly due to the gold tube containers opening during the furnace heating.

By using the reagents of calcium oxide and copper oxide in respectively larger stoichiometric amounts in the  $Tl_2Ba_2Ca_{3-x}Sr_xCu_4O_y$  samples, there were fewer occurrences of experiments that resulted in mixed-phase products. Shorter furnace heating times could be used with a smaller risk of the sample tube containers opening at the high synthesis temperatures. A few  $Tl_2Ba_2Ca_{2.85}Sr_{0.15}Cu_4O_y$  products showed X-ray diffraction patterns that closely resembled the X-ray diffraction

pattern of the ideal 2223 structure.  $T_C$ 's up to 112K were observed in some of these products.

Silver tubing proved to perform nearly as well as gold tubing in experiments where the heating conditions were of lower temperatures and shorter duration. Temperatures up to 875°C for as long as four to five hours could be endured by hermetically-sealed silver tube containers before tube fatigue, opening, or collapse would occur. Studies in the  $Tl_2Ba_2(Ca_{0.85}Sr_{0.15})_{x-1}Cu_xO_y$  system, where both gold and silver tube containers were used, gave results to indicate that products could be made with either tube container and have similar  $T_C$ 's under heating conditions that both gold and silver tube containers could sustain.

After investigating some different strontium-substituted systems that were prepared under various synthesis conditions, the results from the strontium substitutions did not indicate any enhancements in the 2223-type structure or phases responsible for high- $T_C$  behavior. A new research emphasis was then begun to determine exactly what the ideal synthesis techniques and conditions were to produce an ideal non-strontium-substituted 2223 structure. In attempting this, the  $Tl_2Ba_2Ca_{2+x}Cu_{3+x}O_y$  system was studied with a wide range of stoichiometries where  $x$  ranged from 0.1 to 0.9 under a variety of different heating conditions. The stoichiometry of  $Tl_2Ba_2Ca_{2.5}Cu_{3.5}O_y$  had the best results with single-phase three-layer X-ray diffraction patterns and  $T_C$ 's as high as 115K.

With some successes in the  $Tl_2Ba_2Ca_{2.5}Cu_{3.5}O_y$  system, strontium substitution was attempted to study possible trends in phase formation,  $T_C$ , and refined cell dimensions. For these experiments, the system of  $Tl_2Ba_2Ca_{2.5-x}Sr_xCu_{3.5}O_y$  was studied where  $x = 0.1$  to 0.5. The results

indicated no trends of single-phase formation because mixed-phase products were often observed. There were no observed trends of  $T_C$  with respect to strontium substitution, although some of the highest observed  $T_C$ 's were seen consistently in the range of 112K to 117K for these systems. Nonetheless, there was a slight correlation of heating time and  $T_C$ . Samples heated for longer time periods, four hours or more, usually resulted in products that had slightly higher  $T_C$ 's than samples heated for shorter periods (two hours or less). The longer heating periods allowed adequate time for the three-layer phase to form, whereas a short heating period left three-layer phase formation incomplete.

Least-squares cell refinement showed no relationship between changes in sample stoichiometry nor the level of strontium substitution and the  $c$ -axis cell dimension in the  $Tl_2Ba_2Ca_{2+x}Cu_{3+x}O_y$  and  $Tl_2Ba_2Ca_{2.5-x}Sr_xCu_{3.5}O_y$  systems. More importantly, the cell refinement data can be discounted because the calculated standard deviations for the refinements were large enough to render the data statistically insignificant.

Post-synthesis annealing treatment with reducing and oxidizing gases ( $H_2(g)$ ,  $N_2(g)$ , and  $O_2(g)$ ) did not show any enhancements for the three-layer superconducting phases of various products. Low temperature (around  $300^\circ C$ ) and short duration (less than three hours) annealing experiments typically did not result in any observable changes in the X-ray diffraction patterns and measured superconducting critical temperatures. However, high temperature (over  $350^\circ C$ ) or long duration (up to six hours) annealing experiments destroyed or severely diminished the superconducting phases of the products.

The best synthesis conditions found in this study using silver tube containers were, 1) pre-heating the furnace to 865°C, 2) inserting the sealed sample tubes into the furnace for four to six hours, and 3) directly removing the tubes to room temperature. The results in the  $Tl_2Ba_2Ca_{2.5-x}Sr_xCu_{3.5}O_y$  system indicated some of the highest  $T_c$ 's observed in this study (up to 117K) using this synthesis technique. No  $T_c$ 's beyond 117K were ever observed for any product in this study.

Using gold and silver tube containers in hermetically-sealed high-temperature reactions proved to be a great challenge throughout this study. The results from a few systems revealed that longer furnace heating periods helped to better form single-phase three-layer products. However, a major limitation in the duration of the heating periods was the temperature-handling capabilities of the tube containers, especially silver tubing. Many of the sealed tubes opened during high-temperature furnace heating experiments and resulted in mixed-phase products. Interestingly enough, there were some experiments where a sealed tube container did open and some contents of the tube escaped, yet a single-phase, or near-single-phase product was produced. These "seemingly-successful" experiments in which reagents or tube contents escaped were extremely difficult to reproduce because there were no means to determine when the sealed tubes opened, or even how much of the tube contents escaped the tubing during the furnace heating period. Therefore, the reproducibility of experiments was very much limited to a fraction of the experiments where the tube containers stayed sealed throughout the furnace heating period.

## BIBLIOGRAPHY

1. Bednorz, J. G.; Muller, K. A. *Z. Phys.* **B64**, 189 (1986).
2. Wu, M. K.; Ashburn, J. R.; Torng, C. J.; Hor, P. H.; Meng, R. L.; Gao, L.; Huang, Z. J.; Wang, Y. Q.; Chu, C. W. *Phys. Rev. Lett.* **58**, 908 (1987).
3. Michel, C.; Hervien, H.; Borel, M. M.; Grandin, A.; Deslendes, F.; Provost, J.; Raveau, B. *Z. Phys.* **B68**, 421 (1987).
4. Sheng, Z. Z.; Hermann, A. M. *Nature* **332**, 55 (1988).
5. Maeda, H.; Tanaka Y.; Fukutomi, M.; Assano, T. *Jpn. J. Appl. Phys.* **27**, L209 (1988).
6. Sheng, Z. Z.; Hermann, A. M. *Nature* **332**, 138 (1988).
7. Hazen, R. M.; Finger, L. W.; Angel, R. J.; Prewitt C. T.; Ross, N. L.; Hadidiacos, C. G.; Heaney, P. J.; Veblen, D. R.; Sheng, Z. Z.; El Ali, A.; Hermann, A. M. *Phys. Rev. Lett.* **60**, 1657 (1988).
8. Torardi, C. C.; Subramanian, M. A.; Calabrese, J. C.; Gopalakrishnan, J.; Morrissey, K. J.; Askew, T. R.; Flippen, R. B.; Chowdhry, U.; Sleight, A. W. *Science* **240**, 631 (1988).

9. Parkin, S. S. P.; Lee, V. Y.; Engler, E. M.; Nazzal, A. I.; Huang, T. C.; Gorman, G.; Savoy, R.; Beyers, R. *Phys. Rev. Lett.* **60**, 2539 (1988).
10. Kusahara, H.; Kotani, T.; Takei, H.; Tada, K. *Jpn. J. Appl. Phys.* **28**, L1772 (1989).
11. Kikuchi, M.; Nakajima, S.; Syono, Y.; Hiraga, K.; Oku, T.; Shindo, D.; Kobayashi, N.; Iwasaki, H.; Muto, Y. *Physica C* **158**, 79 (1989).
12. Torardi, C. C.; Subramanian, M. A.; Calabrese, J. C.; Gopalakrishnan, J.; McCarron, E. M.; Morrissey, K. J.; Askew, T. R.; Flippen, R. B.; Chowdhry, U.; Sleight, A. W. *Phys. Rev. B.* **38**, 225 (1988).
13. Subramanian, M. A.; Calabrese, J. C.; Torardi, C. C.; Gopalakrishnan, J.; Askew, T. R.; Flippen, R. B.; Morrissey, K. J.; Chowdry, U.; Sleight, A. W. *Nature* **332**, 420 (1988).
14. Shannon, R. D. *Acta Crystallogr.* **A32**, 751-767 (1976).
15. Cox, D. E.; Torardi, C. C.; Subramanian, M. A.; Gopalakrishnan, J.; Sleight, A. W. *Phys. Rev. B.* **38**, 6624 (1988).
16. Subramanian, M. A.; Gai, P. L.; Sleight, A. W. *Mat. Res. Bull.* **25**, 101 (1990).

17. Wada, T.; Kaneko, T.; Yamauchi, H.; Tanaka, S. *ISTEC* 3, 21 (1990).
18. Izumi, F. *Nippon Kessho Gakkai Shi (J. Crystallogr. Soc. Jpn., in Japanese)* 27, 23 (1985).
19. Izumi, F. *Rigaku J.* 6, No. 1, 10 (1989).
20. Izumi, F. Advances in the Rietveld Method. Young, R. A., ed.; Oxford University Press: Oxford, in press (1990).
21. CRC Handbook of Chemistry and Physics, 66th Edition. Weast, R. C., ed.; CRC Press, Inc.: Boca Raton, FL (1985) pp. B-38, B-151.
22. Sleight, A. W. *Phase Transitions* 19, 149 (1989).

## **APPENDICES**

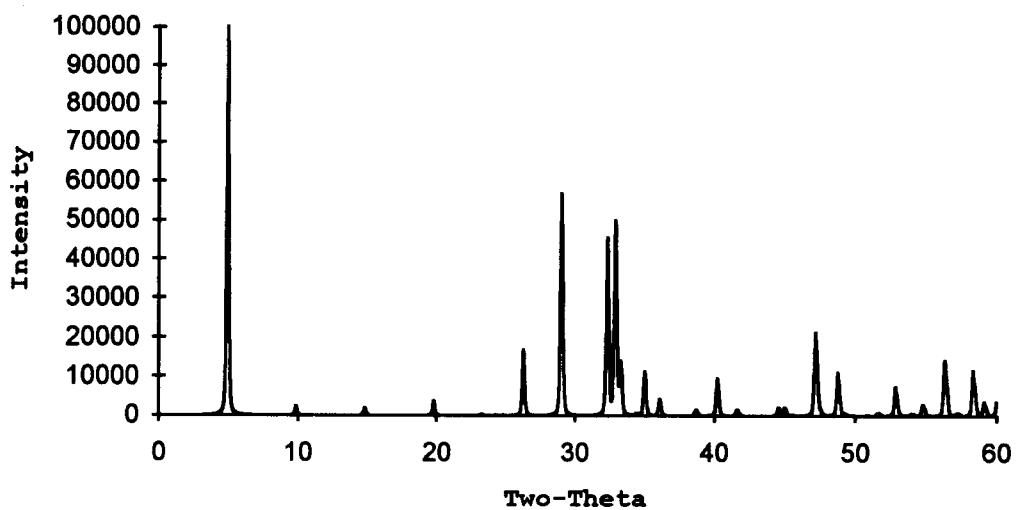
Appendix 1. Theoretical X-ray diffraction pattern of  $\text{Tl}_2\text{Ba}_2\text{Ca}_2\text{Cu}_3\text{O}_{10}$ .

Figure 15. X-ray diffraction pattern of  $\text{Tl}_2\text{Ba}_2\text{Ca}_2\text{Cu}_3\text{O}_{10}$ . This X-ray diffraction pattern was generated using the Rietveld analysis computer program Rietan.<sup>1-3</sup> The atomic parameters used for input data into Rietan were from a 2223 structure determination by Torardi *et al.*<sup>4</sup>

## REFERENCES

1. Izumi, F. *Nippon Kessho Gakkai Shi (J. Crystallogr. Soc. Jpn., in Japanese)* **27**, 23 (1985).
2. Izumi, F. *Rigaku J.* **6**, No. 1, 10 (1989).
3. Izumi, F. Advances in the Rietveld Method. Young, R. A., ed.; Oxford University Press: Oxford, in press (1990).
4. Torardi, C. C.; Subramanian, M. A.; Calabrese, J. C.; Gopalakrishnan, J.; Morrissey, K. J.; Askew, T. R.; Flippen, R. B.; Chowdhry, U.; Sleight, A. W. *Science* **240**, 631 (1988).



The physical significance of equation (2) relates the permeability,  $B/H$ , to magnetic forces. The ratio  $B/H$  can be defined to be:

$$\frac{B}{H} = \frac{\text{density of lines of force within the substance}}{\text{density of lines of force in the same region without the substance}} \quad (3)$$

Thus, volume susceptibility of a vacuum = 0, because by definition,  $B/H$  must = 1 in a vacuum.

Diamagnetic susceptibilities are negative because the induced dipole force lines cancel out some applied magnetic field force lines. By similar reasoning, paramagnetic susceptibilities are positive because the magnetic flux is greater within the substance than in a vacuum.

Mass magnetic susceptibility is related to the volume magnetic susceptibility by:

$$X_m = X / d \quad (4)$$

where:  $X_m$  = mass magnetic susceptibility  
 $X$  = volume magnetic susceptibility  
 $d$  = mass density of the substance

If the density is not known for the substance, the following equation can be used in the case of a Lake Shore 7000 AC Susceptometer mass magnetic susceptibility measurement:

$$X_m = \frac{a v}{m f H} \quad (5)$$

where:

- m = mass of substance
- v = measured RMS voltage (at the susceptometer coils)
- a = calibration coefficient
- f = frequency of alternating current field
- H = RMS magnetic field

When properly initialized, the software of the Lake Shore 7000 AC Susceptometer only requires the user to input mass data during sample measurements. The other variables in equation (5) are inherently known via the software. As a result, all output data is in terms of mass magnetic susceptibility.

## REFERENCES

1. Cotton, F. A.; Wilkinson, G. Advanced Inorganic Chemistry, Fourth Edition. John Wiley & Sons, Inc.: New York, N. Y. (1980) pp. 1360-1361.
2. Model 7000 AC Susceptometer Instruction Manual. Lake Shore Cryotronics, Inc. (1989) p. 10.

Appendix 3. Relationship of measured voltage and susceptibility in the  
Lake Shore 7000 AC Susceptometer.

This section briefly describes how the Lake Shore 7000 AC Susceptometer converts measured voltages from its two secondary sensing coils to a single voltage that is used to calculate mass magnetic susceptibility.

The electronic sensitivity of the measurement system exceeds the physical capability to manufacture two identical secondary sensing coils, hence, a slight offset voltage can be measured when no sample is present in the susceptometer. Moving the sample precisely between the two secondary sensing coils and making two voltage measurements allows compensation to be made for the offset voltage.

If the offset voltage is given by  $v_0$ , the top secondary sensing coil,  $S_1$ , will measure a voltage  $v_1$  by the relationship:

$$v_1 = v + v_0 \quad (1)$$

where  $v$  is the true voltage.

When the sample is moved to the bottom secondary sensing coil,  $S_2$ , the coil will measure a voltage  $v_2$  by the relationship:

$$v_2 = -v + v_0 \quad (2)$$

where the voltage is measured negatively with respect to the first sample position because the secondary sensing coils are connected in opposition via a lock-in amplifier. The offset voltage remains constant since it is unaffected by sample movement or to which sensing coil the sample is positioned.

Therefore, the true sample voltage can be determined from the two separate voltage measurements,  $v_1$  and  $v_2$ , by:

$$v = (v_1 - v_2) / 2 \quad (3)$$

where  $v$  is the true voltage of the measurement. This true voltage,  $v$ , is used directly in equation (5) of Appendix 2 to determine mass magnetic susceptibility.

## REFERENCES

1. Model 7000 AC Susceptometer Instruction Manual. Lake Shore Cryotronics, Inc. (1989) p. 5.